

Supporting Information

**Bimetallic Oxidative Addition Involving Radical Intermediates in Nickel-Catalyzed Alkyl-
Alkyl Kumada Coupling Reactions**

Jan Breitenfeld, Jesus Ruiz, Matthew D. Wodrich, and Xile Hu*

Institute of Chemical Sciences and Engineering, Ecole Polytechnique Fédérale de Lausanne (EPFL), ISIC-
LSCI, BCH 3305, Lausanne, CH 1015, Switzerland. E-mail: xile.hu@epfl.ch

Contents

Contents:	2
Table of Figures:	3
General section:.....	5
A. Chemicals and Reagents	5
B. Physical methods	5
Experimental section:.....	6
Radical clock experiment:	6
Stereochemical control experiment for ring closing reaction:.....	8
Synthesis of 9-D:	10
Attempted trapping of alkyl radicals by TEMPO.....	11
Reaction of [(N ₂ N)Ni- ⁿ Pr] with ⁿ C ₄ H ₉ I	15
Reaction of [(N ₂ N)Ni- ⁿ Pr] with ⁿ C ₄ H ₉ I in the presence of ⁿ PrMgCl.....	16
Reaction of [(N ₂ N)Ni- ⁿ Pr] with ⁿ C ₄ H ₉ I in the presence of ⁿ BuLi	17
Reaction of [(N ₂ N)Ni- ⁿ Pr] with ⁿ PrMgCl.....	17
Reaction of [(N ₂ N)Ni- ⁿ Pr] with MeMgCl.....	17
Reaction of [(N ₂ N)Ni- ⁿ Pr]with ⁿ C ₄ H ₉ I and ⁿ C ₄ H ₉ MgCl in the presence of with an excess of TMEDA	18
Reaction of [(N ₂ N)Ni- ⁿ Pr]with ⁿ C ₄ H ₉ I in the presence of MgCl ₂	18
Reaction of [(N ₂ N)Ni- ⁿ Pr] with ⁿ C ₈ H ₁₇ I and ⁿ BuMgCl.....	19
Kinetic Study: Rate order consideration.....	21
Kinetic Study: Dependence on ⁿ BuMgCl.....	21
Kinetic Study: Dependence on catalyst loading.....	23
Kinetic Study: Dependence on substrate.....	24
Kinetic Study: Dependence on a Lewis-base - addition of TMEDA	26
Kinetic Study: Dependence on MgCl ₂	26
Dependence on Schlenk equilibrium – addition of MgCl ₂ to (Bu) ₂ Mg	28
Kinetic Study: Dependence of transmetalation on Grignard reagents.....	30
Reaction of [(N ₂ N)Ni- ⁿ Pr] with <i>tert</i> -Butyl-4-phenylbutaneperoxoate under irradiation	32
Reaction of ⁿ PrMgCl with <i>tert</i> -Butyl-4-phenylbutaneperoxoate under irradiation.....	33
Irradiation of [(N ₂ N)Ni- ⁿ Pr]	36
Irradiation of <i>tert</i> -Butyl-4-phenylbutaneperoxoate	36
Computational details	53

References	59
------------------	----

Table of Figures

Figure S1. The ratio of 12/13 as a function of the loading of the catalyst (1) in the coupling reaction of 9 and ⁿ BuMgCl.....	7
Figure S2. Chromatogram of the radical clock experiment in the presence of TMEDA.....	13
Figure S3. Chromatogram of the reaction of 1 with TEMPO and ⁿ BuMgCl.....	14
Figure S4. Representative stack plot of ¹ H-NMR spectra of the reaction of [(N ₂ N)Ni- ⁿ Pr with ⁿ C ₄ H ₉ I.	15
Figure S5. Representative stack plot of ¹ H NMR spectra of the reaction the reaction of [(N ₂ N)Ni- ⁿ Pr with ⁿ C ₄ H ₉ I in the presence of ⁿ PrMgCl..	16
Figure S6. Stack plot of ¹ H NMR spectra of the reaction of [(N ₂ N)Ni- ⁿ Pr]with ⁿ C ₄ H ₉ I in the presence of MgCl ₂	19
Figure S7. Dependence of C ₁₁ H ₂₄ /C ₁₂ H ₂₆ ratio on the equivalent of ⁿ BuMgCl.....	21
Figure S8. Reaction profile under variable concentrations of ⁿ BuMgCl.	22
Figure S9. Reaction profile under variable concentrations of 1	24
Figure S10. Reaction profile under variable concentrations of substrate.	25
Figure S11. Reaction profile under variable concentrations of MgCl ₂	28
Figure S12. Reaction profile under variable concentrations of ⁿ Bu ₂ Mg/MgCl ₂	29
Figure S13. The change of absorption spectra during transmetalation reactions.....	31
Figure S14. The rate of transmetalation as a function of Grignard concentration.	31
Figure S15. Chromatogram of the reaction of [(N ₂ N)Ni- ⁿ Pr] with <i>tert</i> -Butyl-4-phenylbutaneperoxoate after irradiation.....	32
Figure S16. ¹ H NMR of the reaction mixture of ⁿ PrMgCl with <i>tert</i> -Butyl-4-phenylbutaneperoxoate.....	33
Figure S17. Chromatogram of the product mixture of Reaction of ⁿ PrMgCl with <i>tert</i> -Butyl-4-phenylbutaneperoxoate under irradiation with mass spectrum of the product with the retention time of 5.4.	34
Figure S18. Chromatograph and mass spectrum of hexylbenzene.	35
Figure S19. ¹ H NMR of [(N ₂ N)Ni- ⁿ Pr] before irradiation and after irradiation.....	36
Figure S20. ¹ H NMR of <i>tert</i> -Butyl-4-phenylbutaneperoxoate before irradiation and after irradiation.	37

Figure S21. Chromatogram of <i>tert</i> -Butyl-4-phenylbutaneperoxoate after irradiation.	37
Figure S22. Absorption spectra of reaction mixture during a catalytic coupling of octyl iodide with EtMgCl.	39
Figure S23. ¹ H NMR (400 MHz, CDCl ₃) spectrum of 12	40
Figure S24. ¹ H NMR (400 MHz, CDCl ₃) spectrum of 13	40
Figure S25. ¹³ C{ ¹ H} NMR (100 MHz, CDCl ₃) spectrum of 13	41
Figure S26. Chromatogram of the independently synthesized sample of 12	41
Figure S27. Mass spectrum of the independently synthesized sample of 12	42
Figure S28. Chromatogram of the isolated sample of 13	42
Figure S29. Mass spectrum of the isolated sample of 13	43
Figure S30. Chromatograph of the products from the coupling reactions shown in Scheme 2; both 12 and 13 can be identified by the retention time.	43
Figure S31. Mass spectrum of 12 produced from the coupling reactions shown in Scheme 2.	44
Figure S32. Mass spectrum of 13 produced from the coupling reactions shown in Scheme 2.	44
Figure S33. ¹ H NMR (400 MHz, CDCl ₃) spectrum of 22	45
Figure S34. ¹ H NMR (400 MHz, CDCl ₃) spectrum of 9-D	45
Figure S35. ¹³ C{ ¹ H} NMR (100 MHz, CDCl ₃) spectrum of 9-D	46
Figure S36. ² H NMR (60 MHz, CDCl ₃) spectrum of 9-D	46
Figure S37. ¹ H NMR (800 MHz, C ₆ D ₆) spectrum of 14	47
Figure S38. ¹³ C{ ¹ H} NMR (200 MHz, C ₆ D ₆) spectrum of 14	47
Figure S39. ¹ H NMR (800 MHz, C ₆ D ₆) spectrum of 14-D	48
Figure S40. ¹³ C{ ¹ H} NMR (200 MHz, C ₆ D ₆) spectrum of 14-D with expansion of signals showing diastereomers.	48
Figure S41. ² H NMR (60 MHz, CDCl ₃) spectrum of 14-D	49
Figure S42. Expansion of ¹ H NMR (800 MHz, C ₆ D ₆) signals of 14-D (top) and 14 (bottom).	49
Figure S43. COSY NMR (800MHz, C ₆ D ₆) spectrum of 14-D	50
Figure S44. HMQC NMR (800MHz, C ₆ D ₆) spectrum of 14-D	50
Figure S45. ¹ H NMR (400 MHz, C ₆ D ₆) spectrum of 13-D	51
Figure S46. ¹³ C{ ¹ H} NMR (100 MHz, C ₆ D ₆) spectrum of 13-D with expansion of broad signals indicating diastereomers.	51
Figure S47. ² H NMR (60 MHz, CDCl ₃) spectrum of 13-D	52

General section:

A. Chemicals and Reagents

All manipulations were carried out under an inert N₂(g) atmosphere using standard Schlenk or glovebox techniques. Solvents were purified using a two-column solid-state purification system (Innovative Technology, NJ, USA) and transferred to the glove box without exposure to air. Deuterated solvents were purchased from Cambridge Isotope Laboratories, Inc., and were degassed and stored over activated 3 Å molecular sieves. All other reagents were purchased from commercial sources and were degassed by standard freeze-pump-thaw procedures prior to use. The following chemicals were prepared according to procedures in the literature: complex [(N₂N)Ni-Cl] (**1**),¹ and [(N₂N)Ni-ⁿPr] ,² substrates 3-(2-bromoethoxy)prop-1-ene (**9**),³ 2-(prop-2-ynoxy)ethanol,⁴ 2-(prop-2-yn-1-yloxy)ethyl toluenesulfonate (**21**),⁵ *tert*-Butyl-4-phenylbutaneperoxoate.⁶

B. Physical methods

The ¹H, ¹³C{¹H}, ²H, COSY, and HMQC NMR spectra were recorded on a Bruker Avance 400 spectrometer or on a Bruker Avance II 800 spectrometer. ¹H NMR chemical shifts were referenced either to residual solvent as determined relative to Me₄Si (δ = 0 ppm) or to Me₄Si directly. GC measurement was conducted on a Perkin-Elmer Clarus 400 GC with a FID detector. GC-MS measurements were conducted on a Perkin-Elmer Clarus 600 GC equipped with Clarus 600T MS and a FID detector. Photochemical experiments were performed in a Rayonet Photochemical Reactor, using Rayonet Photochemical Reactor Lamps of 2537 Å for homogenic irradiation of the samples. The internal temperature was maintained within a 40-60 °C range with the aid of an integrated mechanical ventilation system. Absorption spectra were recorded with a Hellma Excalibur UV-vis fiber optic probe connected to a Varian 50 Bio UV-Vis spectrometer.

Experimental section:

Radical clock experiment:

Remark: In a typical experiment, five reactions (five different concentrations of **1**) were run simultaneously in order to maintain identical reaction conditions and to assure the quality of the data.

Prior to the experiments, the following standard solutions were prepared and the concentration of ⁿBuMgCl (2 M) was checked by literature method prior to use:⁷

(A) A solution of [(N₂N)Ni-Cl] (174.3 mg, 0.5 mmol, 0.1 M) in 5 mL DMA was used to prepare five solutions, each with a total volume of 1 mL DMA and 0.01 mmol (2 mol%), 0.02 mmol (4 mol%), 0.035 mmol (7 mol%), 0.5 mmol (10 mol%), or 0.075 mmol (15 mol%) of **1**, respectively.

(B) A solution of 3-(2-bromoethoxy)prop-1-ene (412.5 mg, 2.5 mmol, 1 M) and C₁₀H₂₂ (355 mg, 2.5 mmol, 1 M) in 2.5 mL DMA.

Inside the glovebox, five vials were charged with one of the previously prepared solutions of A (**1**) (vide supra, 15 mol% - 2 mol%), 0.5 mL of solution B (0.5 mmol 3-(2-bromoethoxy)prop-1-ene/0.5 mmol C₁₀H₂₂ and cooled to -20°C.

Method I) Slow addition of Grignard:

After 5 min, ⁿBuMgCl (2M in THF, 0.3 mL, 0.6 mmol) was added slowly to each vial by syringe pump with stirring. After the addition was complete, the solution was stirred for another 30 minutes. The reaction was quenched with water (5 mL), extracted with diethyl ether (2 x 10 mL), dried over Na₂SO₄ and filtered. The yields, the conversions and the ratios were obtained by GC-MS using C₁₀H₂₂ as internal standard (the FID detector was used for the quantification). The results are shown in Figure 2, main text. For an example GC chromatogram see Figure S30.

Method II) Fast addition of Grignard:

To ensure a high coupling yield, we initially added Grignard reagent slowly (see above). As the addition rate of ⁿBuMgCl might have an influence on the ratio of **12/13**, we repeated the experiment and added ⁿBuMgCl at once. The reaction time, workup and sample preparation were the same as before. The results are shown in Figure S1. The same linear dependence of **12/13** as a function of the loading of the

catalyst (**1**) was observed, as in Figure 2 (main text), while the total yield dropped from average 90% to about 30%. A higher amount of C_8H_{18} was found (~15%), due to the homocoupling of Grignard reagent.

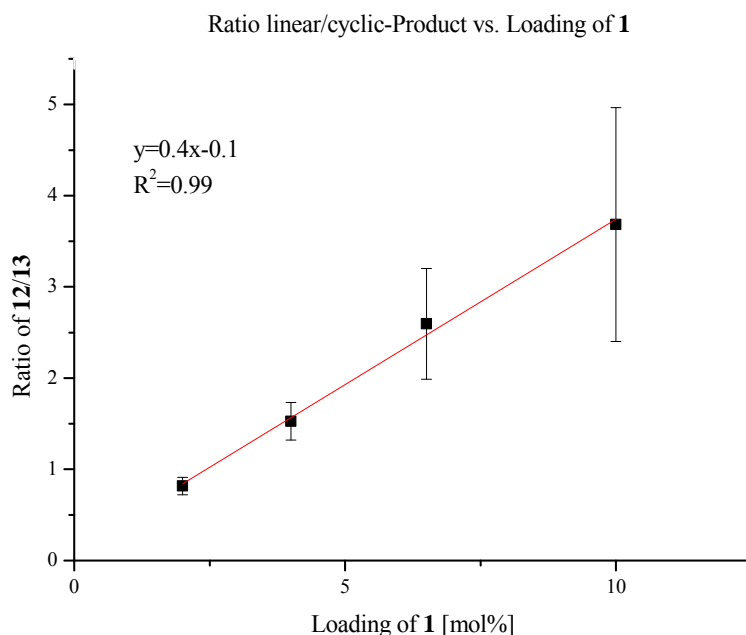


Figure S1. The ratio of **12/13** as a function of the loading of the catalyst (**1**) in the coupling reaction of **9** and $nBuMgCl$, when $nBuMgCl$ was added at once. At each loading, 3 independent trials were conducted to obtain an averaged ratio.

Identification of products:

The identity of the linear product **12** was confirmed by comparison of spectroscopic data (GC and GC-MS) with an independently synthesized sample:

1-hexanol (3.25 g, 31.8 mmol) was dissolved in THF under N_2 atmosphere at $0^\circ C$. NaH (1.72 g, 41.3 mmol, 1.3 equiv.) was added and the solution was stirred for 10 min. at $0^\circ C$. After adding allyl bromide (5.00 g, 41.3 mmol, 1.3 equiv.), the solution was then allowed to stir for 30 min at room temperature and reflux overnight. The reaction was quenched by the addition of saturated ammonium chloride solution. The mixture was then extracted with diethyl ether (3 x 50 mL) and the organic phase was washed with brine (3 x 50 mL), water (2 x 50 mL) and dried over Na_2SO_4 . The solvent was removed by rotary evaporation. The crude product was purified by vacuum distillation to afford **12** as a colorless oil. Yield:

1.8 g (40%).

^1H NMR (400.13 MHz, CDCl_3) δ 5.91 (ddt, $J = 17.4, 10.7, 5.5$ Hz, 1H), 5.26 (dd, $J = 17.2, 1.9$ Hz, 1H), 5.16 (d, $J = 10.4$ Hz, 1H), 3.95 (d, $J = 5.6$ Hz, 2H), 3.41 (t, $J = 6.7$ Hz, 2H), 1.57 (p, $J = 6.8$ Hz, 2H), 1.41 - 1.23 (m, 6H), 0.88 (t, $J = 6.6$ Hz, 3H). ^{13}C $\{^1\text{H}\}$ NMR (101 MHz, CDCl_3) δ 135.1, 116.6, 71.8, 70.5, 31.7, 29.7, 25.9, 22.6, 14.0. The NMR data match those in the literature.⁸

NMR, GC, and MS data for **12** are shown in Figures S23, 26, 27, 31.

The cyclic product **13** was isolated after catalysis under the following conditions:

A vial was charged with 3-(2-bromoethoxy)prop-1-ene (500 mg, 3.03 mmol) and **1** (50 mg, 0.143 mmol, 5 mol%) in 10 mL DMA. The solution was cooled to -20°C , and $^n\text{BuMgCl}$ in THF (2 M, 1.8 mL, 3.6 mmol) was added slowly with a syringe pump while stirring. The reaction was quenched after 1 h by addition of water (15 mL). Then diethyl ether (15 mL) was added. The organic layer was separated and the aqueous layer extracted with diethyl ether (3 x 10 mL). The combined organic layers were dried over Na_2SO_4 , filtered and the solvent was removed by rotary evaporation. After purification by preparative TLC using hexane/ethyl acetate (10/1) **13** was isolated as colorless oil. Yield: 25 mg (6%).

^1H NMR (400.13 MHz, CDCl_3) δ 3.93 – 3.67 (m, 3H), 3.30 (t, $J = 7.8$ Hz, 1H), 2.15 (dt, $J = 14.6, 7.3$ Hz, 1H), 2.01 (dtd, $J = 12.1, 7.3, 4.6$ Hz, 1H), 1.47 (dq, $J = 12.0, 7.9$ Hz, 1H), 1.33 (ddd, $J = 22.8, 12.2, 7.7$ Hz, 8H), 0.87 (t, $J = 6.8$ Hz, 3H). ^{13}C $\{^1\text{H}\}$ NMR (101 MHz, CDCl_3) δ . 73.64, 68.10, 39.55, 33.41, 32.67, 32.10, 28.41, 22.73, 14.18.

NMR, GC, and MS data for **13** are shown in Figures 24, 25, 28, 29, 32.

Stereochemical control experiment for ring closing reaction:

To distinguish a radical mechanism from a non-radical path such as the one involving concerted oxidative addition, intramolecular olefin insertion into a metal-alkyl bond, and reductive elimination, we examined the reaction of **9** and **9-D** with $^n\text{BuMgCl}$ or phenethylmagnesium chloride and isolated the cyclic product **13-D** or **14** and **14-D**. The change of Grignard to phenethylmagnesium chloride simplified both the NMR analysis and the purification by preparative TLC, as the molecule is UV-vis active. In contrast, **13** and **13-D**, are not UV-active. The reaction conditions for the synthesis of **13-D** were identical to those of **13** (see above). NMR data of **13-D** are shown in Figures S45-47.

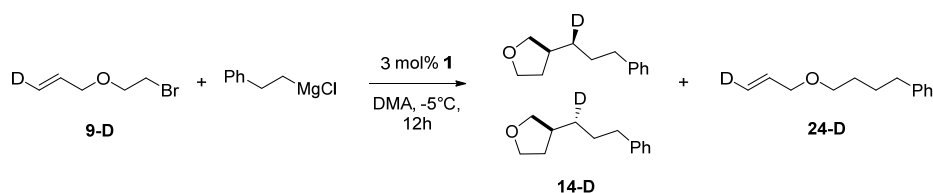
For the reaction of **9** and **9-D** with phenethylmagnesium chloride:

A vial was charged with **9** or **9-D** (300 mg, 1.84 mmol) and **1** (20 mg, 0.057 mmol, 3 mol%) in 2 mL DMA. The solution was cooled to -5°C , and a mixture of phenethylmagnesium chloride (1 M, 3 mL, 3

mmol) and TMEDA (200 mg, 1.72 mmol; added to increase the yield) in THF was added slowly with a syringe pump over 2 h while stirring. The reaction was stirred overnight at -5°C and then at room temperature for additional 30 min. The reaction was quenched by addition of water (15 mL). Then pentane (50 mL) was added. The organic layer was separated and the aqueous layer extracted with pentane (3 x 50 mL). The combined organic layers were dried over Na₂SO₄, filtered and the solvent was removed by rotary evaporation. After purification by preparative TLC using hexane/ethyl acetate (10/1) **14** or **14-D** was isolated as colorless oil. Yield: 28 mg (8%).

14 : ¹H NMR (800 MHz, C₆D₆) δ 7.21 – 7.17 (m, 2H, CH_{Aryl}), 7.11 – 7.08 (m, 1H, CH_{Aryl}), 7.07 – 7.04 (m, 2H, CH_{Aryl}), 3.82 – 3.77 (m, 1H, CHCH₂O), 3.71 (td, *J* = 8.2, 4.6 Hz, 1H, CH₂CH₂O), 3.61 (dd, *J* = 15.6, 7.6 Hz, 1H, CH₂CH₂O), 3.23 – 3.20 (m, 1H, CHCH₂O), 2.43 – 2.35 (m, 1H, CH₂Ph), 1.84 – 1.77 (m, 1H, CH₂CHCH₂), 1.62 (dtd, *J* = 12.1, 7.6, 4.6 Hz, 1H, OCH₂CH₂CH), 1.43 – 1.31 (m, 2H, PhCH₂CH₂), 1.15 – 1.07 (m, 3H, OCH₂CH₂CH and PhCH₂CH₂CH₂). ¹³C NMR (201 MHz, C₆D₆) δ 142.65, 128.71, 128.66, 126.14, 73.41, 67.83, 39.58, 36.35, 33.19, 32.69, 30.72.

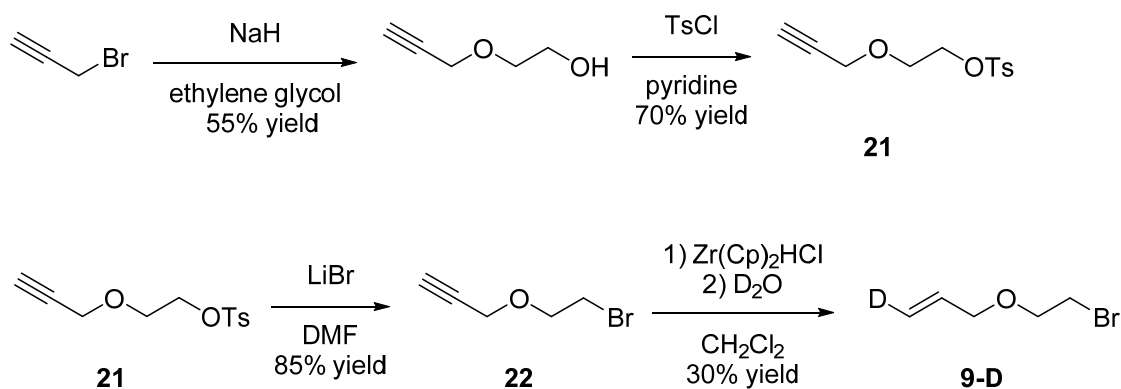
14-D : ¹H NMR (800 MHz, C₆D₆) δ 7.21 – 7.17 (m, 2H, CH_{Aryl}), 7.09 (t, *J* = 7.4 Hz, 1H, CH_{Aryl}), 7.07 – 7.03 (m, 2H, CH_{Aryl}), 3.81 – 3.77 (m, 1H, CHCH₂O), 3.70 (td, *J* = 8.2, 4.6 Hz, 1H, CH₂CH₂O), 3.61 (dd, *J* = 15.5, 7.7 Hz, 1H, CH₂CH₂O), 3.23 – 3.19 (m, 1H, CHCH₂O), 2.43 – 2.34 (m, 1H, CH₂Ph), 1.84 – 1.76 (m, 1H, CH₂CHCH₂), 1.65 – 1.59 (m, 1H, OCH₂CH₂CH), 1.42 – 1.30 (m, 2H, PhCH₂CH₂), 1.15 – 1.05 (m, 2H, OCH₂CH₂CH and PhCH₂CH₂CH₂). ¹³C NMR (201 MHz, C₆D₆) δ 142.66, 128.71, 128.66, 126.13, 73.41, 73.39, 73.38, 67.82, 67.82, 39.49, 36.33, 32.78 (1:1:1,t, ¹*J*_{CD} = 19 Hz), 32.67, 32.66, 30.62. ²H NMR (61 MHz, C₆D₆) δ 1.06.



NMR data for **14** are shown in Figures S37, 38, 42.

NMR data for **14-D** are shown in Figures S39-44.

Synthesis of 9-D:



3-(2-bromoethoxy)prop-1-yne (**22**):

Powdered LiBr (9.38 g, 108 mmol, 3eq) was added to a stirred solution of **21** (9.18 g, 36.0 mmol) in 70 mL dry DMF at 0°C. The reaction mixture was allowed to reach room temperature and was stirred overnight. Then water (200 mL) and hexane (250 mL) were added. The organic phase was separated and the aqueous phase extracted with hexane (3 x 150 mL). The combined organic phase was washed with water, brine (each 2 x 100 mL), dried by MgSO₄ and the solvent was removed by rotary evaporation. After purification by column chromatography using hexane/ethyl acetate (3/1), **22** was isolated as a colorless oil. Yield: 5.10 g (85%). The NMR data match those in the literature.

¹H NMR (400.13 MHz, CDCl₃) δ 4.23 (d, *J* = 2.4 Hz, 2H), 3.86 (t, *J* = 6.1 Hz, 2H), 3.50 (t, *J* = 6.1 Hz, 2H), 2.46 (t, *J* = 2.4 Hz, 1H).

NMR data for **22** are shown in Figure S 33.

(*E*)-1-deuterio-3-(2-bromoethoxy)prop-1-ene (**9-D**):

The compound was synthesized following a slightly modified literature strategy.⁹ In the dark, compound **22** (2.3 g, 0.014 mol 1 eq.) was dissolved in 15 mL of CH₂Cl₂ and added drop wise to a white suspension of Cp₂ZrHCl (Schwartz's reagent, 5.0 g, 0.017 mol, 1.2 eq.) in 25 mL of CH₂Cl₂. The reaction mixture was stirred at room temperature for 4 hours in the dark, during which it turned into a clear orange solution. The solution was transferred out of the glove box in a septum-covered round bottomed flask. Then D₂O (7 mL) was added to this solution, causing the orange color to immediately disappear. The solution was stirred at room temperature for 60 minutes. The reaction mixture was then

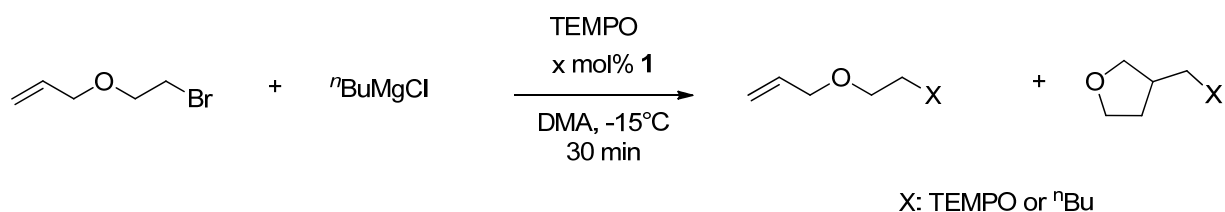
diluted with about 40 mL of diethyl ether, causing a white solid to precipitate. The solution was dried over magnesium sulfate, filtered through a plug of silica, and concentrated. After purification by distillation at reduced pressure, **9-D** was isolated as colorless oil. Yield: 0.70 g (30%). The product was contaminated with ca. 5% of the (*E*)-2-deuterio-3-(2-bromoethoxy)prop-1-ene isotopomer. The NMR properties are consistent with those reported for the non-deuterated analogue.¹⁰

¹H NMR (400.13 MHz, CDCl₃) δ 5.89 (dt, *J* = 17.1, 5.5 Hz, 1H), 5.27 (d, *J* = 17.2 Hz, 1H), 4.13 – 3.96 (m, 2H), 3.74 (t, *J* = 6.2 Hz, 2H), 3.46 (t, *J* = 6.2 Hz, 2H); ¹³C NMR (101 MHz, CDCl₃) δ 134.26, 117.34 (1:1:1,t, ¹*J*_{CD} = 24 Hz) 72.10 (1:1:1,t, ³*J*_{CD} = 2 Hz), 70.02, 30.46; ²H NMR (61 MHz, CDCl₃) δ 5.24 (d, ²*J*_{HD} = 1.5 Hz).

NMR data for **9-D** are shown in Figures S34-36.

Attempted trapping of alkyl radicals by TEMPO:

In order to support our hypothesis that an alkyl radical stemming from the alkyl halide is leaving the solvent cage, we thought of trapping it by TEMPO. If the latter reacts with the alkyl radical it would furnish either a linear or a cyclic product. The radical clock experiment was therefore repeated at constant loading of **1** and varying the concentration of TEMPO under the following conditions:



Remark: In a typical experiment, five reactions (five different concentrations of TEMPO) were run simultaneously in order to maintain identical reaction conditions and to assure the quality of the data. Prior to the experiments, the following standard solutions were prepared and the concentration of ⁿBuMgCl (2 M) was checked by literature method prior to use:⁷

(A) A solution of [(N₂N)Ni-Cl] (34.8 mg, 0.0999 mmol, 0.05 M) in 10 mL DMA.

(B) A solution of 3-(2-bromoethoxy)prop-1-ene (412.5 mg, 2.5 mmol, 0.5 M) and C₁₀H₂₂ (355 mg, 2.5 mmol, 0.5 M) in 5.0 mL DMA.

(C) ⁿBuMgCl (0.2M, 50 mL THF), the concentration was checked by literature method prior to use.⁷

(D) TEMPO (117.0 mg, 0.74 mmol, 0.5 M) in 1.5 mL THF. Then five solutions with a total volume of 0.5 mL were prepared containing 0.05 mmol, 0.1 mmol, 0.15 mmol, 0.2 mmol, and 0.25 mmol of TEMPO (THF was used to dilute), respectively.

Inside the glovebox, five vials were charged with 0.1 mL of solutions of **A** (2 mol%, 0.005 mmol of **1**), 0.5 mL of solution **B** (0.25 mmol 3-(2-bromoethoxy)prop-1-ene/0.25 mmol C₁₀H₂₂), one of the solutions of **D** (vide supra, TEMPO 0.05 – 0.25 mmol), and cooled to – 20°C. After 5 min, ⁿBuMgCl (0.2M in THF, 0.15 mL, 0.3 mmol) was added slowly to each vial by syringe pump with stirring. After the addition was complete, the solution was stirred for another 30 minutes. Then an aliquot (60 µL) was collected and immediately transferred into a GC vial, containing (60 µL) acetonitrile to quench the reaction. After addition of 1 mL of Et₂O the sample was analyzed by GC-MS. The yields, the conversions and the ratios were obtained by GC-MS using C₁₀H₂₂ as internal standard (the FID detector was used for the quantification). A representative chromatogram is depicted in Figure S2. The results are summarized in Table S 1. For all five TEMPO concentrations the ratio of **12/13** as well as the yield was almost the same (~0.9 and ~20 %). No coupling product between **10** or **11** and TEMPO was detected. The major signal was identified as a product of TEMPO with [(N₂N)Ni-ⁿBu] (from reaction of [(N₂N)Ni-Cl] with ⁿBuMgCl). The latter was confirmed by an independent synthesis (identical reaction condition of entry 5 in the absence of **9**; the chromatogram is shown in Figure S3. Similar results have been already reported for stoichiometric reactions of [(N₂N)Ni-Me] with CH₂Cl₂ in the presence of TEMPO.¹

$${}^n\text{BuMgCl} + \mathbf{9} + \text{TEMPO} \xrightarrow{2 \text{ mol}\% \mathbf{1}} \mathbf{12} + \mathbf{13} + \text{TEMPO-}{}^n\text{Bu}$$

x equiv

entry	Equiv. of TEMPO	conversion of 9 (%)	yield of 12+13 (%)	Ratio 12/13	conversion of TEMPO (%)	Yield TEMPO-Bu (%)
1	0.2	31	22	0.9	81	11
2	0.4	31	23	0.9	78	21
3	0.6	29	25	0.9	78	31
4	0.8	29	25	0.8	82	43
5	1.0	33	20	0.8	85	59

Table S 1. Results of radical clock experiment in presence of TMEDA.

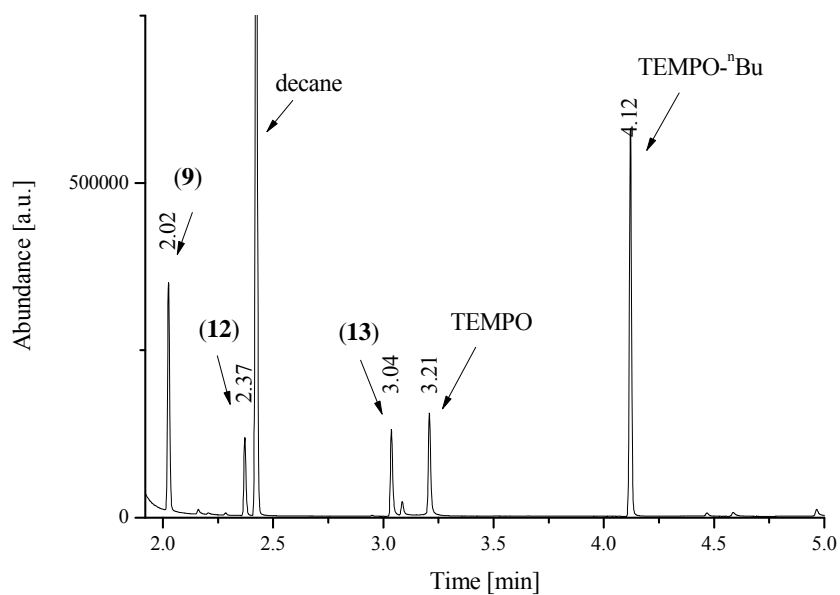


Figure S2. Chromatogram of the radical clock experiment in the presence of TMEDA (entry 5).

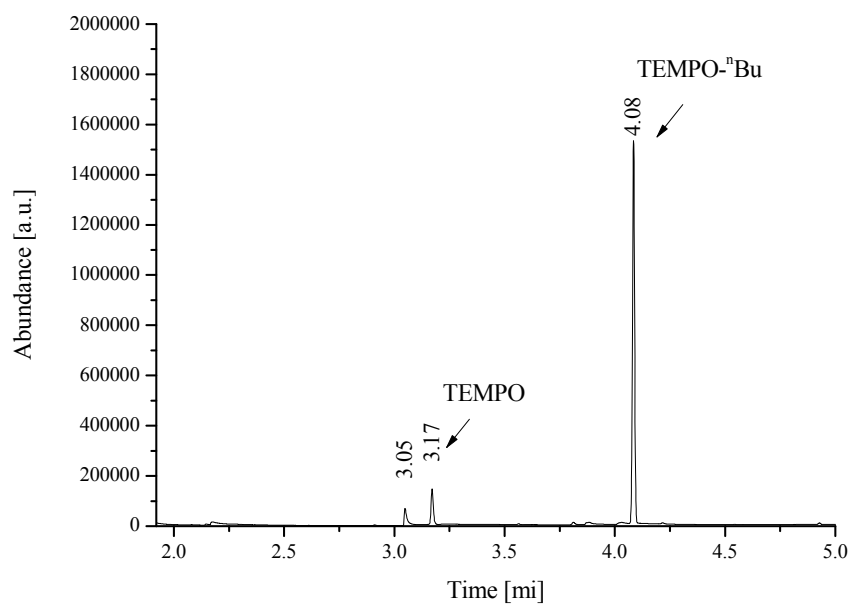


Figure S3. Chromatogram of the reaction of **1** with TEMPO and ⁿBuMgCl.

Reaction of $[(N_2N)Ni-^{13}Pr]$ with $^{13}C_4H_9I$

In a typical experiment, an air free NMR tube with septum screw cap was charged with a solution of $[(N_2N)Ni-^{13}Pr]$ (5.3 mg, 0.015 mmol) in 1 mL solvent (THF- d_8 , DMA or DMA/THF 0.7 mL/0.3 mL mixture) inside the glovebox. The tube was transferred to the spectrometer and a 1H NMR spectrum was recorded at $-15^\circ C$. The sample was ejected and $^{13}C_4H_9I$ (27.6 mg, 0.15 mmol, 10 equiv.) was quickly added by a Hamilton syringe (100 μL). In case of need, the spectrometer was shimmed again and the reaction was periodically monitored (every 15 min) over night by 1H -NMR at $-15^\circ C$. The progress of the reaction was followed by integration of the α - CH_2 signal (~ -0.5 ppm, depending on solvent) attached to the nickel versus the internal standard (TMS, 0.0 ppm) (Figure S4). The half-life of the reaction was determined to be 6 h. No dependence on the solvent was observed.

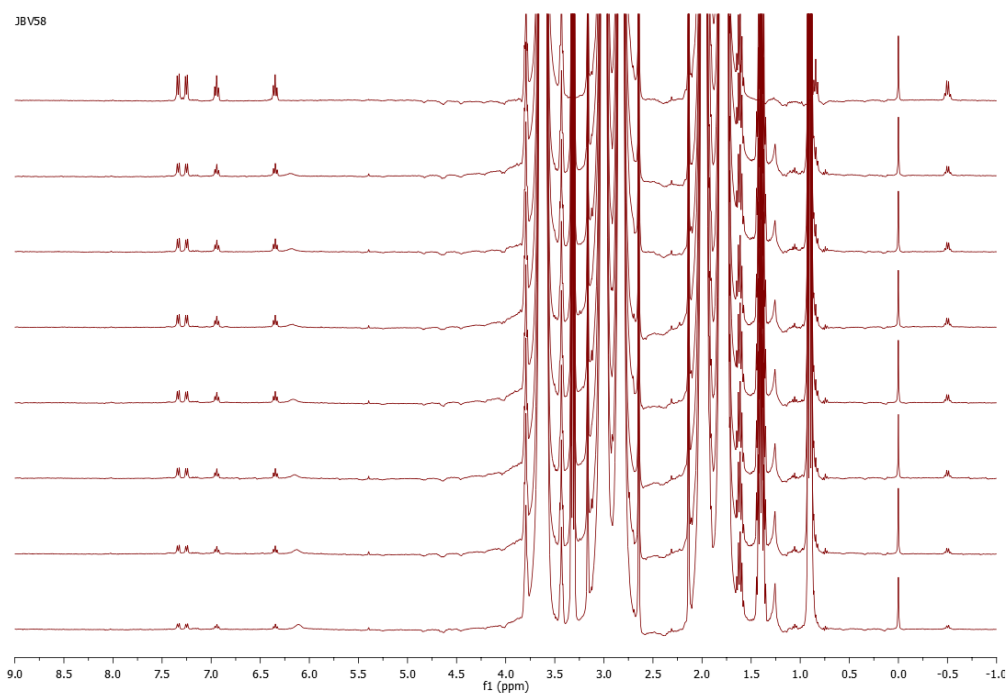


Figure S4. Representative stack plot of 1H -NMR spectra (DMA/THF at $-15^\circ C$) of the reaction of $[(N_2N)Ni-^{13}Pr]$ with $^{13}C_4H_9I$. (top) $t=0$; (bottom) after 11 h; $t(1/2) = 6$ h.

Reaction of [(N₂N)Ni-ⁿPr] with ⁿC₄H₉I in the presence of ⁿPrMgCl

In a typical experiment, an air free NMR tube with septum screw cap was charged with a solution of [(N₂N)Ni-ⁿPr] (5.3 mg, 0.015 mmol) in 1 mL solvent (THF-d₈, DMA or DMA/THF 0.7 mL/0.3 mL mixture) inside the glovebox. The tube was transferred to the spectrometer and a ¹H NMR spectrum was recorded at -15°C. The sample was ejected. Then ⁿC₄H₉I (27.6 mg, 0.15 mmol, 10 equiv.) and ⁿPrMgCl (9 μL, 0.018 mmol) were added consecutively and quickly by a Hamilton syringe (10 μL). In case of need the spectrometer was shimmed again. The progress of the reaction was followed by integration of the α-CH₂ signal (~ -0.5 ppm depending on solvent) attached to the nickel versus the internal standard (TMS, 0.0 ppm) (Figure S5). No characteristic signal of [(N₂N)Ni-ⁿPr] was observed after 5 min. No dependence on the solvent was observed.

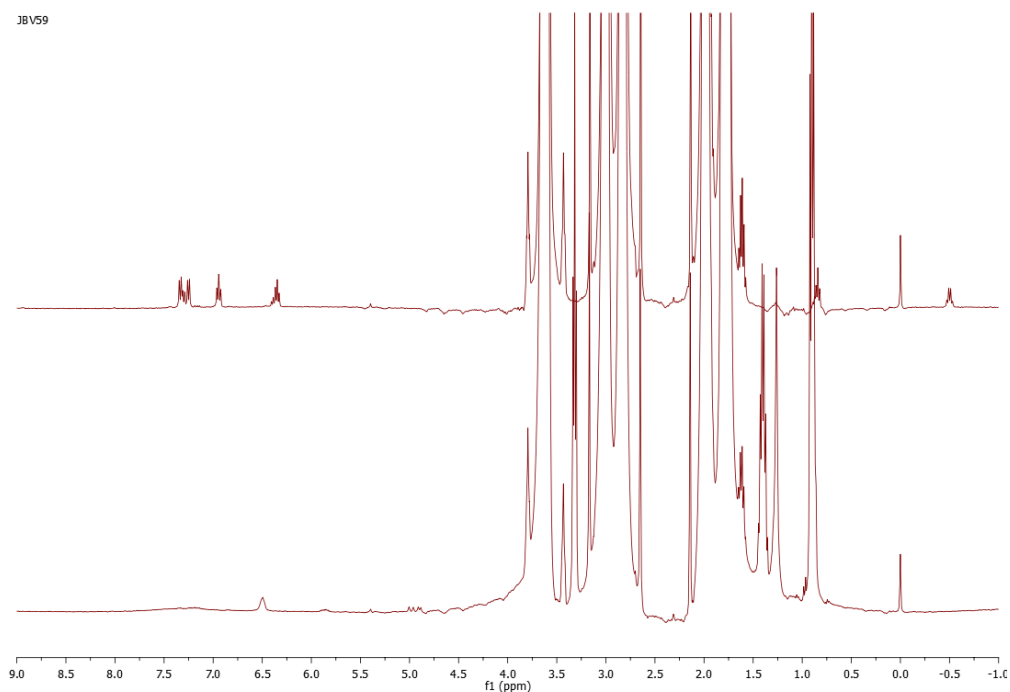


Figure S5. Representative stack plot of ¹H NMR spectra (DMA/THF at -15°C) of the reaction the reaction of [(N₂N)Ni-ⁿPr] with ⁿC₄H₉I in the presence of ⁿPrMgCl. (top) t=0; (bottom) 5 min.

Reaction of [(N₂N)Ni-ⁿPr] with ⁿC₄H₉I in the presence of ⁿBuLi

An air free NMR tube with septum screw cap was charged with a solution of [(N₂N)Ni-ⁿPr] (5.3 mg, 0.015 mmol) in 1 mL THF-d₈, inside the glovebox. The tube was transferred to the spectrometer and a ¹H NMR spectrum was recorded at -15°C. The sample was ejected. Then ⁿC₄H₉I (27.6 mg, 0.15 mmol, 10 equiv.) and ⁿBuLi (10 μL, 0.018 mmol) were added consecutively and quickly by a Hamilton syringe (10 μL). In case of need the spectrometer was shimmed again. The reaction was periodically (every 15 min) monitored by ¹H-NMR at -15°C. The progress of the reaction was followed by integration of the α-CH₂ signal (~ -0.5 ppm depending on solvent) attached to the nickel versus the internal standard (TMS, 0.0 ppm). The half-life of the reaction was determined to be 6 h. No dependence on the solvent was observed.

Reaction of [(N₂N)Ni-ⁿPr] with ⁿPrMgCl

An air free NMR tube with septum screw cap was charged with [(N₂N)Ni-ⁿPr] (5.3 mg, 0.015 mmol) in 1 mL of THF-d₈ inside the glovebox. The tube was transferred to the spectrometer and a ¹H NMR spectrum was recorded at -15°C. The sample was ejected. Then ⁿPrMgCl (9 μL, 0.018 mmol) was added quickly by a Hamilton syringe (10 μL). In case of need the spectrometer was shimmed again. The reaction was periodically (every 15 min) monitored by ¹H-NMR at -15°C. The progress of the reaction was followed by integration of the α-CH₂ signal (~ -0.5 ppm depending on solvent) attached to the nickel versus the internal standard (TMS, 0.0 ppm). No reaction was observed during 12h.

Reaction of [(N₂N)Ni-ⁿPr] with MeMgCl

An air free NMR tube with septum screw cap was charged with [(N₂N)Ni-ⁿPr] (5.3 mg, 0.015 mmol) in 1 mL of THF-d₈ inside the glovebox. The tube was transferred to the spectrometer and a ¹H NMR spectrum was recorded at -15°C. The sample was ejected. Then MeMgCl (9 μL, 0.018 mmol) was added quickly by a Hamilton syringe (10 μL). In case of need the spectrometer was shimmed again. The reaction was periodically (every 15 min) monitored by ¹H-NMR at -15°C. The progress of the reaction was followed by integration of the α-CH₂ signal (~ -0.5 ppm depending on solvent) attached to the nickel versus the internal standard (TMS, 0.0 ppm). No reaction was observed during 12h.

Reaction of [(N₂N)Ni-ⁿPr]with ⁿC₄H₉I and ⁿC₄H₉MgCl in the presence of with an excess of TMEDA

An air free NMR tube with septum screw cap was charged with [(N₂N)Ni-ⁿPr] (5.3 mg, 0.015 mmol) in 1 mL of DMA/THF mixture (0.7 mL/0.3 mL) inside the glovebox. The tube was transferred to the spectrometer and a ¹H NMR spectrum was recorded at -15°C. The sample was ejected. Then ⁿC₄H₉I (27.8 mg, 0.15 mmol, 10 equiv.) and ⁿBuMgCl (9 μL, 0.018 mmol, 1.2 equiv.), pre-mixed with TMEDA (22 μL, 27.5 mg, 0.23 mmol, 15 equiv.) was added consecutively and quickly by a Hamilton syringe (100 μL). In case of need the spectrometer was shimmed again. The progress of the reaction was followed by integration of the α-CH₂ signal (~ -0.5 ppm depending on solvent) attached to the nickel versus the internal standard (TMS, 0.0 ppm). The results were the same as the results obtained for reactions without TMEDA (see above). Thus, in stoichiometric reaction TMEDA does not inhibit the coupling reaction; only in catalytic reactions TMEDA slows down the catalysis.

Reaction of [(N₂N)Ni-ⁿPr]with ⁿC₄H₉I in the presence of MgCl₂

An air free NMR tube with septum screw cap was charged with [(N₂N)Ni-ⁿPr] (5.3 mg, 0.015 mmol) and MgCl₂ (1.4 mg, 0.015 mmol) in 1 mL of DMA/THF mixture (0.7 mL/0.3 mL) inside the glovebox. The tube was transferred to the spectrometer and a ¹H NMR spectrum was recorded at -15°C. The sample was ejected. Then ⁿC₄H₉I (27.8 mg, 0.15 mmol of 10 equiv.) was added quickly by a Hamilton syringe (10 μL). In case of need the spectrometer was shimmed again. The reaction was periodically (every 20 min) monitored by ¹H-NMR at -15°C. The progress of the reaction was followed by integration of the α-CH₂ signal (~ -0.5 ppm depending on solvent) attached to the nickel versus the internal standard (TMS, 0.0 ppm). The half-live of the reaction was determined to be 2 h. Because the final NMR spectrum differed from the one without MgCl₂ additive (Figure S6), we removed all volatiles by vacuum pump and dissolving of the solids in C₆D₆. The ligand containing product was determined by ¹H NMR (C₆D₆); it matched those of [(N₂N)Mg-Cl(THF)].

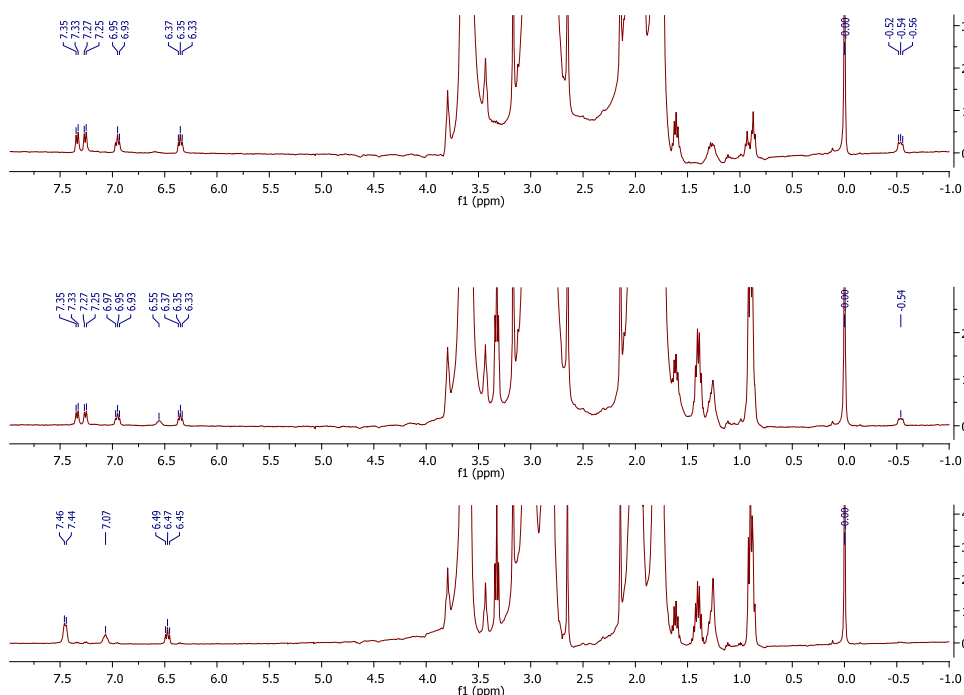


Figure S6. Stack plot of ^1H NMR spectra (DMA/THF at -15°C) of the reaction of $[(\text{N}_2\text{N})\text{Ni}-^{\text{Pr}}]$ with $^{13}\text{C}_4\text{H}_9\text{I}$ in the presence of MgCl_2 . (top) $t=0$; (middle) after addition of $^{13}\text{C}_4\text{H}_9\text{I}$; (bottom) after 4h.

Reaction of $[(\text{N}_2\text{N})\text{Ni}-^{\text{Pr}}]$ with $^{13}\text{C}_8\text{H}_{17}\text{I}$ and $^{\text{n}}\text{BuMgCl}$

Remark: In a typical experiment, four reactions (four different concentrations of $^{\text{n}}\text{BuMgCl}$) were run simultaneously in order to maintain identical reaction conditions and assure the quality of the data. Prior to the experiments, the following standard solutions were prepared:

(A) $[(\text{N}_2\text{N})\text{Ni}-^{\text{Pr}}]$ (95.8 mg, 0.269 mmol, 0.027 M) in 10 mL THF/DMA (5 mL/5mL);

(B) $\text{C}_8\text{H}_{17}\text{I}$ (120 mg, 0.500 mmol, 0.050 M) with $\text{C}_{10}\text{H}_{22}$ (66.5 mg, 0.468 mmol, 0.047 M) in 10 mL DMA;

(C) $^{\text{n}}\text{BuMgCl}$ (0.04 M, 10 mL THF), the concentration was checked by literature method prior to use.⁷

Then four solutions with a total volume of 1 mL were prepared containing 0.02 mmol, 0.015 mmol, 0.010 mmol, and 0.0050 mmol $^{\text{n}}\text{BuMgCl}$ (THF was used to dilute), respectively.

Method I): Normal addition

Inside the glovebox, four vials were charged with 0.74 mL of solution A (0.020 mmol of $[(\text{N}_2\text{N})\text{Ni}-^{\text{Pr}}]$) and cooled to -20°C . Then 0.40 mL of solution B (0.020 mmol $\text{C}_8\text{H}_{17}\text{I}$ /0.019 mmol $\text{C}_{10}\text{H}_{22}$) were added.

After 5 min, to each vial one of the previously prepared ⁿBuMgCl solutions (0.02 mmol - 0.0050 mmol) was added (vide supra). The solutions were stirred for 30 minutes at -20°C. Then an aliquot (40 μL) was collected and immediately transferred into a GC vial containing 60 μL of acetonitrile to quench the reaction. 1 mL of diethyl ether was then added. The yields, conversions and the ratios were obtained by GC-MS using C₁₀H₂₂ as internal standard (the FID detector was used for the quantification).

Method II): Inverse addition

We also tested the influence of the mixing sequence on the ratio of C₁₁H₂₄/C₁₂H₂₆. The later might be influenced by a possible exchange of ⁿBu moiety of the Grignard reagent with ⁿPr moiety of [(N₂N)Ni-ⁿPr] complex before coupling event. Therefore inside the glovebox four vials were charged with 0.74 mL of solution A (0.020 mmol of [(N₂N)Ni-ⁿPr]) and cooled to -20°C. Then one of the previously prepared ⁿBuMgCl solutions was added (see above). The solutions were stirred for 30 min at -20°C. At last, solution 0.40 mL of solution B was added. The reaction time, workup and sample preparation were the same as before. The results are shown in Figure S7. The same trend of C₁₁H₂₄/C₁₂H₂₆ ratio as a function of the equivalent of ⁿBuMgCl was observed. While the total yield dropped from average 90% to about 30%. A higher amount of C₈H₁₈ was present (~15%), due to the homocoupling of Grignard reagent.

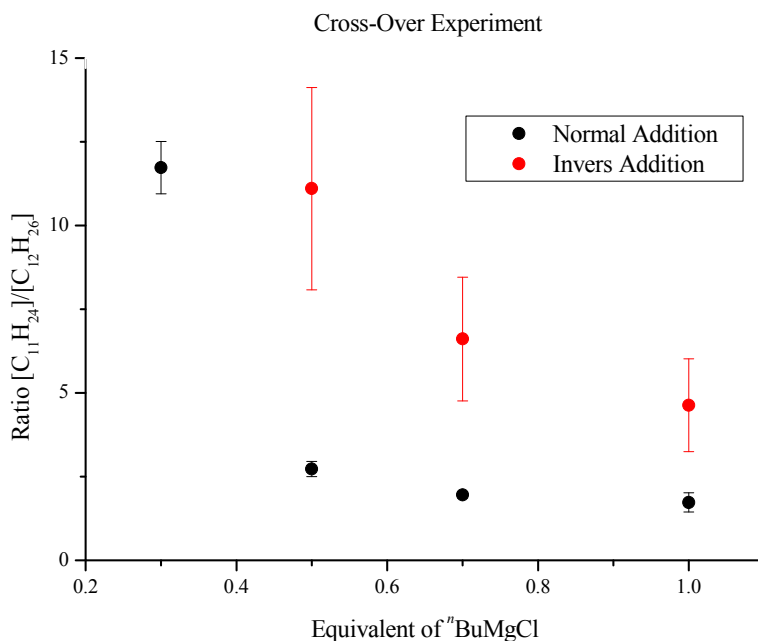


Figure S7. Dependence of C₁₁H₂₄/C₁₂H₂₆ ratio on the equivalent of ⁿBuMgCl; the values are averaged over 3 trials; black: method I) and red: method II).

Kinetic Study: Rate order consideration

The reaction rate r is determined by the initial rate method. $r = k[\text{Ni}]^a[\text{Alkyl}^1\text{-X}]^b[\text{Alkyl}^2\text{-MgX}]^c$. If the concentration of one reagent is varied while the concentrations of the other two are maintained during the measurement, then $r = m[\text{X}]^n$, where m is a constant, and n is the order for the reagent X. $\log r = \log m + n \log[\text{X}]$. The slope of $\log r$ vs. $\log[\text{X}]$ then gives the order of the reaction, n .

Kinetic Study: Dependence on ⁿBuMgCl

Remark: In a typical experiment, five reactions (five different concentrations of ⁿBuMgCl) were run consecutively in order to maintain identical reaction conditions and assure the quality of the data. Prior to the experiments, the following standard solutions were prepared:

(A) [(N₂N)Ni-Cl] (140.0 mg, 0.402 mmol, 0.020 M) in 20 mL DMA;

(B) (2-Bromoethyl)benzene (463 mg, 2.50 mmol, 0.25 M) with C₁₀H₂₂ (355 mg, 2.50 mmol, 0.25 M) in 10 mL THF;

(C) ⁿBuMgCl (0.5M, 10 mL THF), the concentration was checked by literature method prior to use.⁷ Then five solutions with a total volume of 1.5 mL were prepared containing 0.75 mmol, 0.60 mmol, 0.45 mmol, 0.30 mmol, and 0.15 mmol of ⁿBuMgCl (THF was used to dilute), respectively.

Inside the glovebox, five vials with new rubber septum were charged with 0.5 mL of solution A (0.01 mmol, 4mol% of $[(N_2N)Ni-Cl]$), 1.0 mL of solution B (0.25 mmol (2-Bromoethyl)benzene/0.25 mmol $C_{10}H_{22}$) and 1 mL DMA. The vials were transferred outside the glovebox and the following procedure applied to one after the other: One vial placed inside a cooling bath at $-20^\circ C$ (ice/salt) under N_2 atmosphere (pierced by needle) for 3 min with stirring. The septum was removed while N_2 flow was maintained and an aliquot (60 μL) was collected and immediately transferred into a GC vial containing 60 μL of acetonitrile. Then one of the previously prepared nBuMgCl solution (vide supra) was added quickly while stirring. Every 10 seconds an aliquot (60 μL) was collected and immediately transferred into a GC vial containing (60 μL) acetonitrile to quench the reaction. After 90 seconds, the reaction was stopped and 1 mL of Et_2O was added to each GC samples. The yields and the conversions were obtained by GC using $C_{10}H_{22}$ as internal standard.

The obtained kinetic data (Figure S8) was analyzed by initial rates method, with the assumption that data up to a maximum of 10% yield can be used. Based on the latter, the data of the concentration of product vs. time plot was fitted linear with Excel. The obtained slope of the linear fitting represents the reaction rate. The order of monoalkyl-Grignard was derived from a linear fit of the $\log(\text{rate})$ vs. $\log([^nBuMgCl])$ plot. The final data consists of 3 independent trails for each experiment.

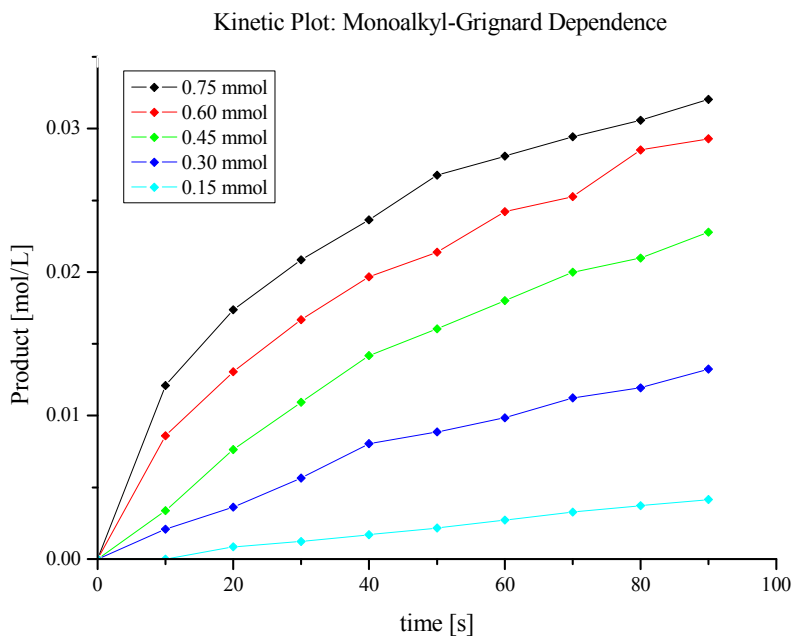


Figure S8. Reaction profile under variable concentrations of nBuMgCl .

Kinetic Study: Dependence on catalyst loading

Remark: In a typical experiment, five reactions (five different concentrations of [(N₂N)Ni- Cl]) were run consecutively in order to maintain identical reaction conditions and ascertain the quality of the data. Prior to the experiments, the following standard solutions were prepared:

(A) [(N₂N)Ni- Cl] (104.6 mg, 0.300 mmol, 0.015 M) in 20 mL DMA. Then five solution with a total volume of 1.5 mL were prepared containing 0.0225 mmol (9 mol%), 0.0175 mmol (7 mol%), 0.0125 mmol (5 mol%), 0.0075 mmol (3 mol%), and 0.0025 mmol (1 mol%) of **1** (DMA was used to dilute), respectively.

(B) (2-Bromoethyl)benzene (936 mg, 5.06 mmol, 0.25 M) with C₁₀H₂₂ (710 mg, 5.00 mmol, 0.25 M) in 10 mL THF;

(C) ⁿBuMgCl (0.2M, 50 mL THF), the concentration was checked by literature method prior to use.⁷

Inside the glovebox, five vials with new rubber septum were charged with one of the previously prepared solutions of A (**1**) (vide supra, 9 mol% - 1 mol%) and 1.0 mL of solution B (0.25 mmol (2-Bromoethyl)benzene/0.25 mmol C₁₀H₂₂). The vials were transferred outside the glovebox and the following procedure applied to one after the other: One vial placed inside a cooling bath at - 20°C (ice/salt) under N₂ atmosphere (pierced by needle) for 3 min with stirring. The septum was removed while N₂ flow was maintained and an aliquot (60 μL) was collected and immediately transferred into a GC vial, containing 60 μL of acetonitrile. Then 1.5 mL of solution C was added quickly while stirring. Every 10 seconds, an aliquot (60 μL) was collected and immediately transferred into a GC vial containing (60 μL) acetonitrile to quench the reaction. After 90 seconds, the reaction was stopped and 1 mL of Et₂O was added to each GC samples. The yields and the conversions were obtained by GC using C₁₀H₂₂ as internal standard.

The obtained kinetic data (Figure S9) was analyzed by initial rates method, with the assumption that data up to a maximum of 10% yield can be used. Based on the latter, the data of the concentration of product vs. time plot was fitted linear with Excel. The obtained slope of the linear fitting represents the reaction rate. The order of monoalkyl-Grignard was derived from a linear fit of the log(rate) vs. log([**1**]) plot. The final data consists of 3 independent trials for each experiment.

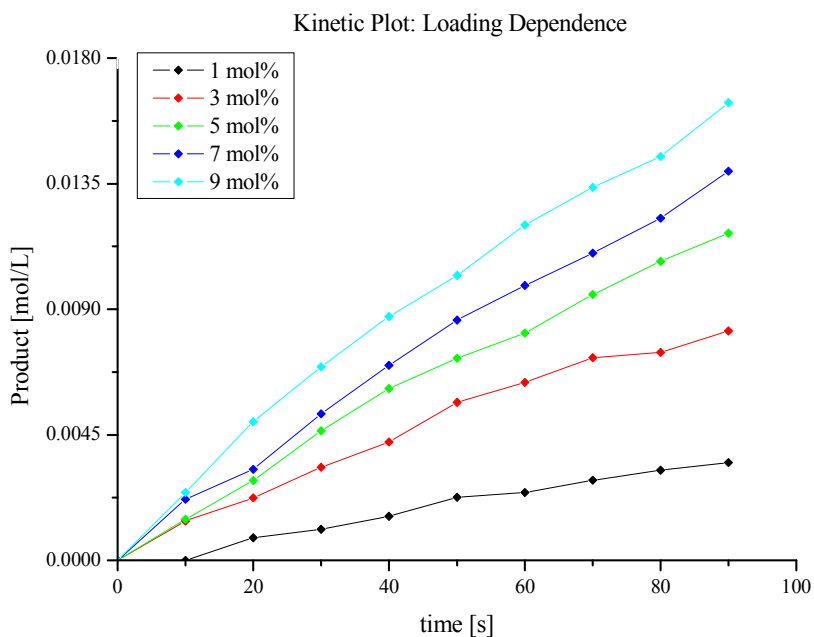


Figure S9. Reaction profile under variable concentrations of **1**.

Kinetic Study: Dependence on substrate

Remark: In a typical experiment, five reactions (five different concentrations of (2-Bromoethyl)benzene) were run consecutively in order to maintain identical reaction conditions and ascertain the quality of the data. Prior to the experiment the following standard solutions were prepared:

(A) $[(N_2N)Ni-Cl]$ (140.0 mg, 0.402 mmol, 0.020 M) in 20 mL THF;

(B) (2-Bromoethyl)benzene (463 mg, 2.50 mmol, 0.25 M) with $C_{10}H_{22}$ (355 mg, 2.50 mmol, 0.25 M) in 10 mL DMA; Then five solution with a total volume of 1.5 mL were prepared containing 0.25 mmol, 0.20 mmol, 0.15 mmol, 0.10 mmol, and 0.050 mmol of (2-Bromoethyl)benzene (DMA was used to dilute), respectively.

(C) $nBuMgCl$ (0.2M, 50 mL THF), the concentration was checked by literature method prior to use.⁷

Inside the glovebox, five vials with new rubber septum were charged with 0.5 mL of solution A (0.01 mmol, 4mol% of $[(N_2N)Ni-Cl]$), one of the previously prepared solutions B (0.25 mmol – 0.050 mmol (2-Bromoethyl)benzene); vide supra) and 2 mL THF. The vials were transferred outside the glovebox and the following procedure applied to one after the other: One vial placed inside a cooling bath at $-20^{\circ}C$ (ice/salt) under N_2 atmosphere (pierced by needle) for 3 min with stirring. The septum was removed while N_2 flow was maintained and an aliquot (60 μ L) was collected and immediately transferred

into a GC vial containing 60 μL of acetonitrile. Then 1.5 mL of solution *C* was added quickly while stirring. Every 10 seconds, an aliquot (60 μL) was collected and immediately transferred into a GC vial, containing (60 μL) acetonitrile to quench the reaction. After 90 seconds, the reaction was stopped and 1 mL of Et_2O was added to each GC samples. The yields and the conversions were obtained by GC using $\text{C}_{10}\text{H}_{22}$ as internal standard.

The obtained kinetic data (Figure S10) was analyzed by initial rates method, with the assumption that data up to a maximum of 10% yield can be used. Based on the latter, the data of the concentration of product vs. time plot was fitted linear with Excel. The obtained slope of the linear fitting represents the reaction rate. The order of monoalkyl-Grignard was derived from a linear fit of the $\log(\text{rate})$ vs. $\log([\text{(2-Bromoethyl)benzene}])$. The final data consists of 3 independent trials for each experiment.

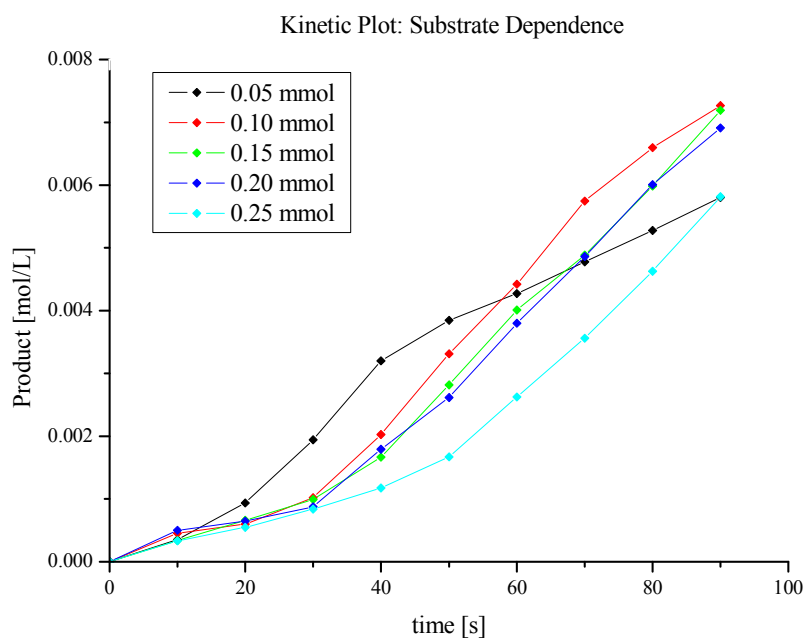


Figure S10. Reaction profile under variable concentrations of substrate.

Kinetic Study: Dependence on a Lewis-base - addition of TMEDA

Remark: In a typical experiment, five reactions (five different concentrations of TMEDA were run consecutively in order to maintain identical reaction conditions and ascertain the quality of the data. Prior to the experiment the following standard solutions were prepared:

(A) [(N₂N)Ni-Cl] (140.0 mg, 0.402 mmol, 0.020 M) in 20 mL DMA;

(B) (2-Bromoethyl)benzene (463 mg, 2.50 mmol, 0.25 M) with C₁₀H₂₂ (355 mg, 2.50 mmol, 0.25 M) in 10 mL THF;

(C) ⁿBuMgCl (0.1M, 50 mL THF), the concentration was checked by literature method prior to use.⁷

Inside the glovebox, five vials with new rubber septum were charged with 0.5 mL of solution A (0.01 mmol, 4mol% of [(N₂N)Ni-Cl]), 1.0 mL of solution B (0.25 mmol (2-Bromoethyl)benzene/0.25 mmol C₁₀H₂₂), 1 ml DMA each. Then different amount of TMEDA was added to each by Hamilton syringe (100 μL) (0 μL, 0 mg, 0 mmol; 10 μL, 7 mg, 0.06 mmol; 20 μL, 14 mg, 0.12 mmol; 30 μL, 21 mg, 0.18 mmol; 40 μL, 28 mg, 0.24 mmol). The vials were transferred outside the glovebox and the following procedure applied to one after the other: One vial placed inside a cooling bath at – 20°C (ice/salt) under N₂ atmosphere (pierced by needle) for 3 min with stirring. The septum was removed while N₂ flow was maintained and an aliquot (60 μL) was collected and immediately transferred into a GC vial containing 60 μL of acetonitrile. Then 1.5 mL of solution C was added quickly while stirring. The first 1.5 min, every 10 seconds, an aliquot (60 μL) was collected and immediately transferred into a GC vial, containing (60 μL) acetonitrile to quench the reaction. A last sample was taken after 30 min reaction time (normally catalysis finishes within 30 min). Then 1 mL of Et₂O was added to each GC samples. The yields and the conversions were obtained by GC using C₁₀H₂₂ as internal standard.

No reaction was observed for all reactions containing TMEDA within the first 90 sec. This is in contrast to the reaction without TMEDA. After 30 min the conversion for all the reactions with TMEDA was ~20%. These results suggest that there is an inhibition due to TMEDA; No dependence on TMEDA was observed within the concentration range measured (6 to 24 equivalents of TMEDA with respect to **1**).

Kinetic Study: Dependence on MgCl₂

Remark: In a typical experiment, five reactions (five different concentrations of MgCl₂ were run consecutively in order to maintain identical reaction conditions and ascertain the quality of the data. Prior to the experiment the following standard solutions were prepared:

(A) [(N₂N)Ni-Cl] (140.0 mg, 0.402 mmol, 0.020 M) in 20 mL DMA;

(B) (2-Bromoethyl)benzene (926 mg, 5.0 mmol, 0.50 M) with C₁₀H₂₂ (710 mg, 5.0 mmol, 0.50 M) in 10 mL THF;

(C) MgCl₂ (40 mg, 0.42 mmol, 0.014M) in 30 mL THF.

(D) ⁿBuMgCl (1.0M, 50 mL THF), the concentration was checked by literature method prior to use.⁷ Then 5 solutions with a total volume of 1.5 mL (THF was used to dilute) were prepared containing 0.3 mL of ⁿBuMgCl (0.3 mmol) each, and 0.0 mmol, 0.004 mmol, 0.008 mmol, 0.013 mmol, and 0.017 mmol of MgCl₂ (from solution C), respectively.

Inside the glovebox, five vials with new rubber septum were charged with 0.5 mL of solution A (0.01 mmol, 4mol% of [(N₂N)Ni-Cl]), 0.5 mL of solution B (0.25 mmol (2-Bromoethyl)benzene/0.25 mmol C₁₀H₂₂), and 1 ml DMA each. The vials were transferred outside the glovebox and the following procedure applied to one after the other: One vial placed inside a cooling bath at – 20°C (ice/salt) under N₂ atmosphere (pierced by needle) for 3 min with stirring. The septum was removed while N₂ flow was maintained and an aliquot (60 μL) was collected and immediately transferred into a GC vial containing 60 μL of acetonitrile to quench the reaction. Then one of the previously prepared ⁿBuMgCl/MgCl₂ solution (vide supra) was added quickly while stirring. Every 10 seconds, an aliquot (60 μL) was collected and immediately transferred into a GC vial, containing (60 μL) acetonitrile to quench the reaction. After 90 seconds, the reaction was stopped and 1 mL of Et₂O was added to each GC samples. The yields and the conversions were obtained by GC using C₁₀H₂₂ as internal standard.

The obtained kinetic data (Figure S11) was analyzed by initial rates method, with the assumption that data up to a maximum of 10% yield can be used. Based on the latter, the data of the concentration of product vs. time plot was fitted linear with Excel. The obtained slope of the linear fitting represents the reaction rate. The final data consists of 2 independent trials for each experiment. An order of approximately 0 was obtained by this method. It appears that MgCl₂ has no influence on the rate of catalysis. Furthermore, it was observed that the addition of MgCl₂ led to a higher amount of (2-chloroethyl)benzene through halogen-exchange.

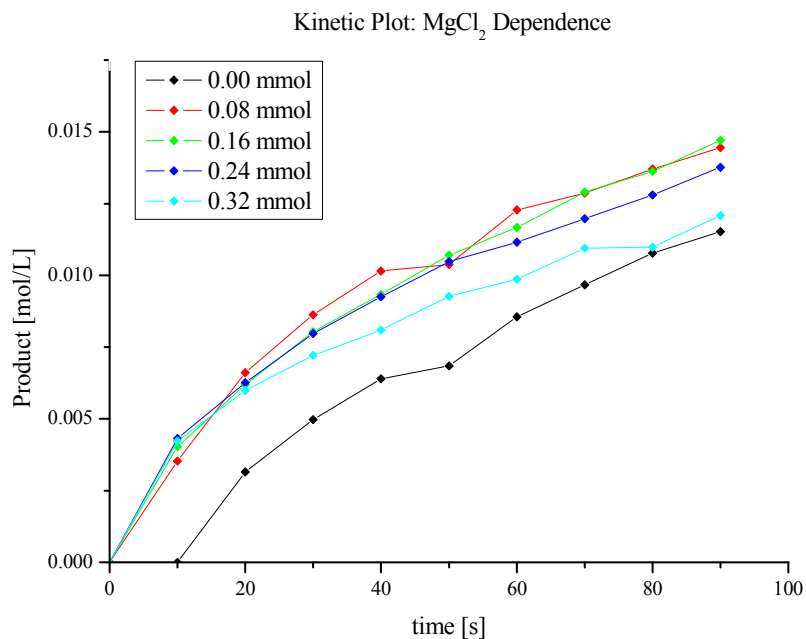


Figure S11. Reaction profile under variable concentrations of MgCl₂.

Dependence on Schlenk equilibrium – addition of MgCl₂ to (Bu)₂Mg

Remark: In a typical experiment, five reactions (five different concentrations of Bu₂Mg/MgCl₂ were run consecutively in order to maintain identical reaction conditions and ascertain the quality of the data. Prior to the experiment the following standard solutions were prepared:

(A) [(N₂N)Ni-Cl] (140.0 mg, 0.402 mmol, 0.020 M) in 20 mL DMA;

(B) (2-Bromoethyl)benzene (926 mg, 5.0 mmol, 0.50 M) with C₁₀H₂₂ (710 mg, 5.0 mmol, 0.50 M) in 10 mL THF;

(C) MgCl₂ (40 mg, 0.42 mmol, 0.014M) in 30 mL THF.

(D) ⁿBu₂Mg (1.0M, heptane), the concentration was checked by literature method prior to use.¹¹ Then 5 solutions with a total volume of 1.5 mL (THF was used to dilute) were prepared containing 0.3 mL of ⁿBu₂Mg (0.3 mmol) each, and 0.0 mmol, 0.004 mmol, 0.008 mmol, 0.013 mmol, and 0.017 mmol of MgCl₂ (from solution C), respectively.

Inside the glovebox, five vials with new rubber septum were charged with 0.5 mL of solution A (0.01 mmol, 4mol% of [(N₂N)Ni-Cl]), 0.5 mL of solution B (0.25 mmol (2-Bromoethyl)benzene/0.25 mmol C₁₀H₂₂), and 1 mL DMA each. The vials were transferred outside the glovebox and the following procedure applied to one after the other: One vial placed inside a cooling bath

at -20°C (ice/salt) under N_2 atmosphere (pierced by needle) for 3 min with stirring. The septum was removed while N_2 flow was maintained and an aliquot ($60\ \mu\text{L}$) was collected and immediately transferred into a GC vial containing $60\ \mu\text{L}$ of acetonitrile to quench the reaction. Then one of the previously prepared ${}^n\text{Bu}_2\text{Mg}/\text{MgCl}_2$ solution (vide supra) was added quickly while stirring. Every 10 seconds, an aliquot ($60\ \mu\text{L}$) was collected and immediately transferred into a GC vial, containing ($60\ \mu\text{L}$) acetonitrile to quench the reaction. After 90 seconds, the reaction was stopped and 1 mL of Et_2O was added to each GC samples. The yields and the conversions were obtained by GC using $\text{C}_{10}\text{H}_{22}$ as internal standard. The obtained kinetic data is represented in Figure S12. No dependence on the Schlenk equilibrium was observed.

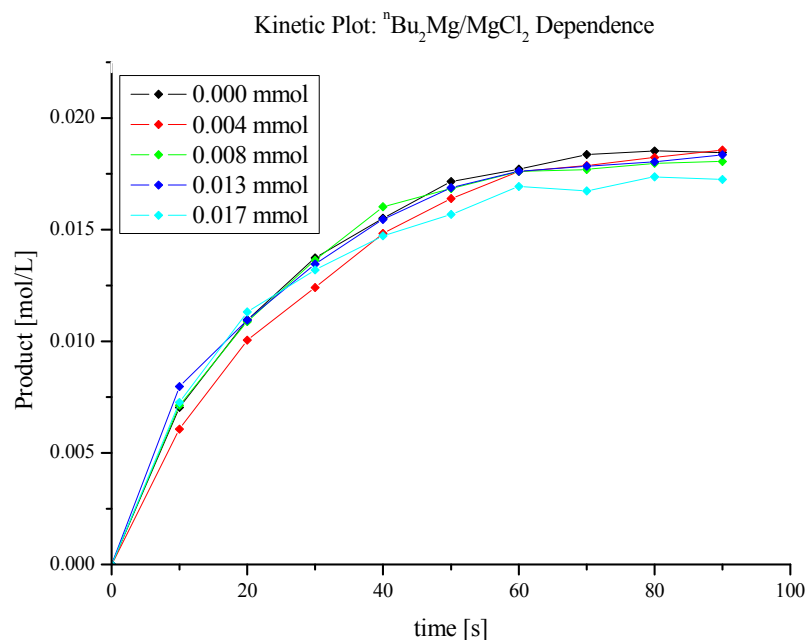


Figure S12. Reaction profile under variable concentrations of ${}^n\text{Bu}_2\text{Mg}/\text{MgCl}_2$

Kinetic Study: Dependence of transmetalation on Grignard reagents

Remark: In a typical experiment, four reactions (four different concentrations of EtMgCl) were run consecutively in order to maintain identical reaction conditions and assure the quality of the data. Prior to the experiments, the following standard solutions were prepared:

(A) [(N₂N)Ni-Cl] (174.3 mg, 0.498 mmol, 0.005 M) in 100 mL THF.

(B) EtMgCl (0.2M, 10 mL THF). The concentration was checked by a literature method prior to use.⁷ Then four solutions with a total volume of 0.25 mL were prepared containing 0.01 mmol, 0.02 mmol, 0.03 mmol, and 0.04 mmol of EtMgCl (THF was used to dilute), respectively.

Inside the glovebox, a brown glass vial was charged with 10 mL of solution A (0.05 mmol, of [(N₂N)Ni-Cl]), a stirring bar, and a Hellma Excalibur UV-vis fiber optic probe (connected to a Varian 50 Bio UV-Vis spectrometer). The solution was cooled to -40°C and the measurements were launched (every 0.03 min a spectrum at 628 nm was recorded during 5 min). After one minute one of the solutions B was added at one.

The obtained kinetic data (Figure S13) was analyzed by initial rates method, using the data where less than 10% decrease in absorbance was observed. The plot of concentration of [(N₂N)Ni-Cl] vs. time was linearly fitted. The slope of this linear fitting represents the initial reaction rate. The order of monoalkyl-Grignard was derived from a linear fit of the log(rate) vs. log([EtMgCl]) plot. The final data consists of 4 independent trails for each experiment. The slope is 1.7 (Figure S14), indicating a rate order close to 2.

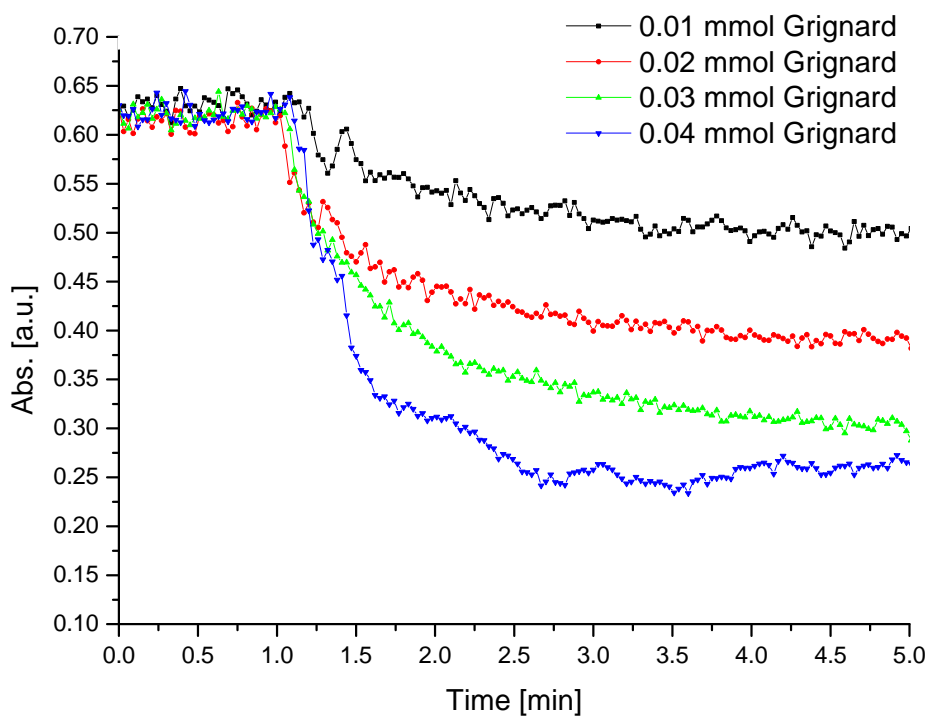


Figure S13. The change of absorption spectra during transmetalation reactions; a different amount of Grignard reagent was applied for each reaction.

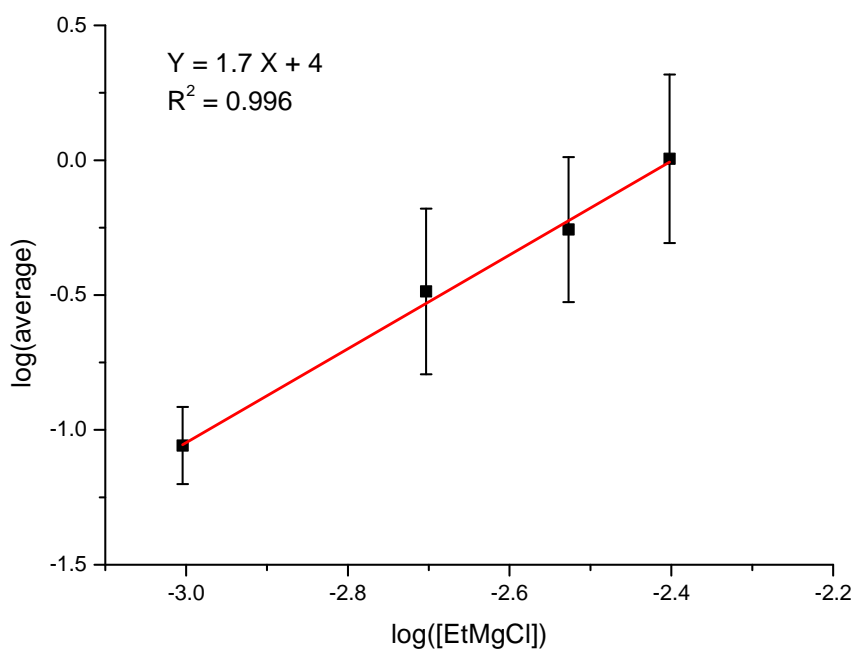


Figure S14. The rate of transmetalation as a function of Grignard concentration. An order of 1.7 is obtained.

Reaction of $[(N_2N)Ni-^{n}Pr]$ with *tert*-Butyl-4-phenylbutaneperoxoate under irradiation

An air free NMR tube with septum screw cap was charged with $[(N_2N)Ni-^{n}Pr]$ (12 mg, 0.034 mmol) and *tert*-Butyl-4-phenylbutaneperoxoate (25 mg, 0.106 mmol, 3 equiv.) and $C_{10}H_{22}$ (8.0 mg, 0.056 mmol) in 2 mL of THF inside the glovebox. The tube was placed in Rayonet Photochemical Reactor. After 2h the solution had turned from red to green. Then an aliquot (60 μ L) was collected and transferred into a GC vial with 1 mL of Et_2O . The yields and the ratios of products were obtained by GC-MS using $C_{10}H_{22}$ as internal standard (the FID detector was used for the quantification). The coupling product was compared to commercial 1-Phenylhexane. An alkylation of the solvent (THF) was also observed. The other products were also found in a blank test (see below, Figure S15). The chromatogram of the reaction of $[(N_2N)Ni-^{n}Pr]$ with *tert*-Butyl-4-phenylbutaneperoxoate (fid) is shown in Figure S15. The Yields for the ^{n}Pr containing products derived from the alkyl moiety of $[(N_2N)Ni-^{n}Pr]$ were calculated to be 14% for compound (a) and 13% for compound (c).

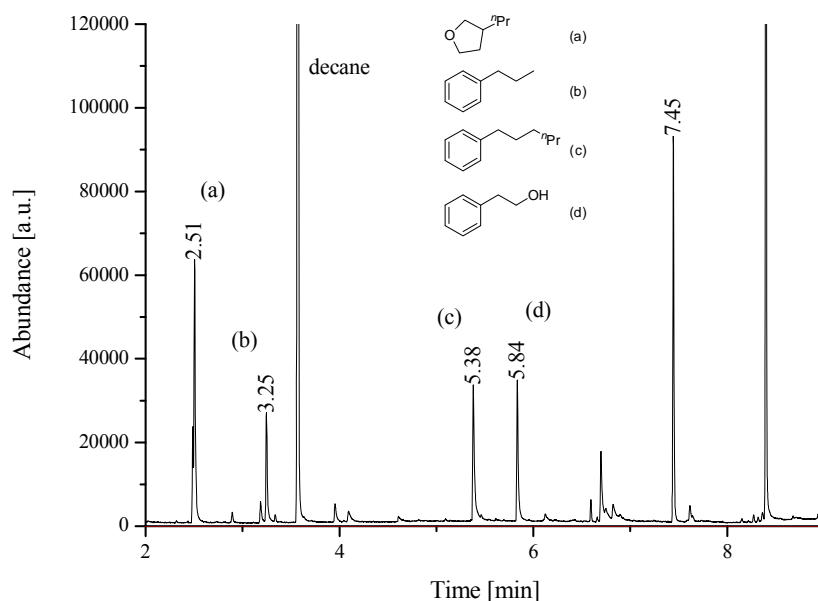


Figure S15. Chromatogram of the reaction of $[(N_2N)Ni-^{n}Pr]$ with *tert*-Butyl-4-phenylbutaneperoxoate after irradiation.

Reaction of ${}^n\text{PrMgCl}$ with *tert*-Butyl-4-phenylbutaneperoxoate under irradiation

An air free NMR tube with a septum screw cap was charged with *tert*-Butyl-4-phenylbutaneperoxoate (6.3 mg, 0.027 mmol) and 25 μL of ${}^n\text{PrMgCl}$ (2M, Et_2O) in 0.5 mL of THF-d_8 inside the glovebox. The tube was transferred to the spectrometer and a ${}^1\text{H}$ NMR spectrum was recorded. The sample was ejected and placed in a Rayonet Photochemical Reactor. After 2h a ${}^1\text{H}$ NMR spectrum was recorded proving that all *tert*-Butyl-4-phenylbutaneperoxoate reacted. The NMR spectra are depicted in Figure S16. Then an aliquot (60 μL) was collected and transferred into a GC vial with 1 mL of Et_2O . The products were probed by GC-MS (Figure S17). No hexylbenzene (coupling of ${}^n\text{PrMgCl}$ with phenylpropyl radical) was observed (see Figure S18 for the spectra of an authentic sample).

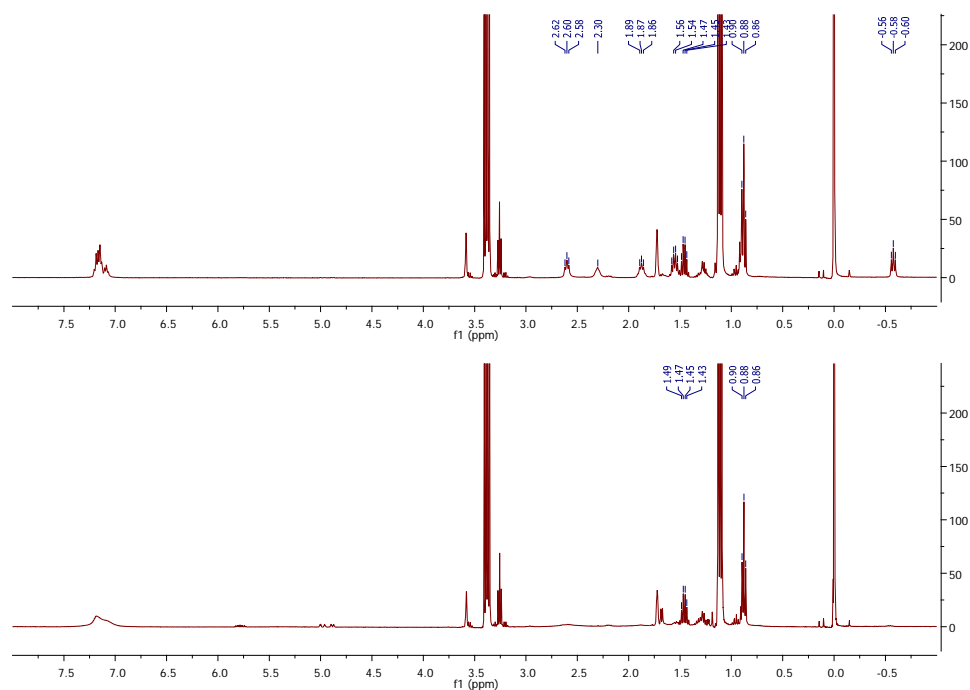


Figure S16. ${}^1\text{H}$ NMR (THF-d_8) of the reaction mixture of ${}^n\text{PrMgCl}$ with *tert*-Butyl-4-phenylbutaneperoxoate; (top) before and (bottom) after irradiation.

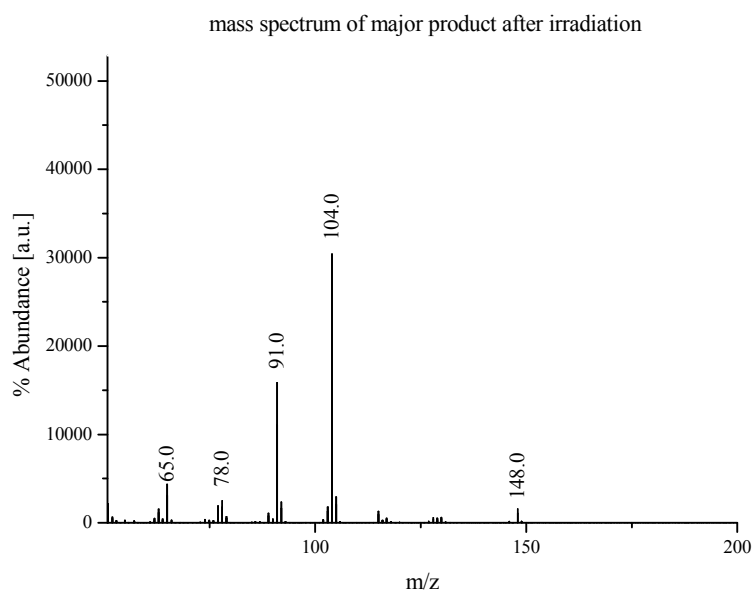
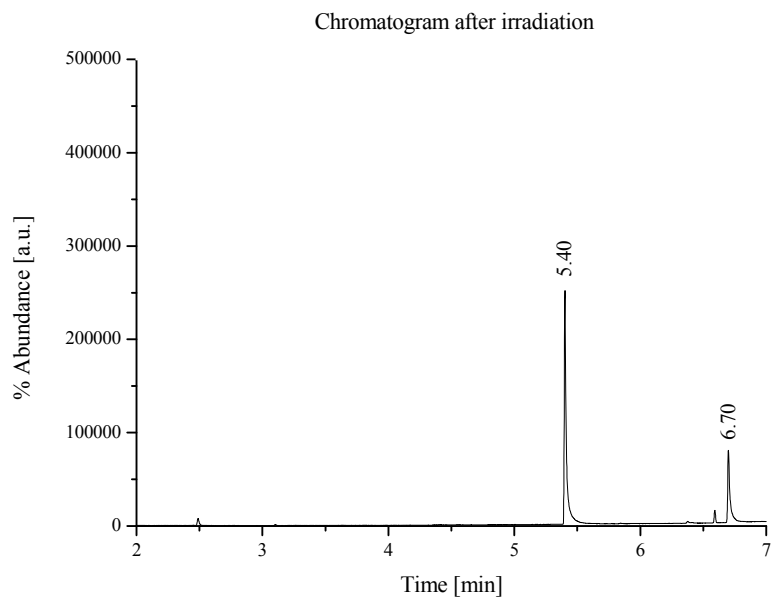


Figure S17. (top) Chromatogram of the product mixture of Reaction of ${}^n\text{PrMgCl}$ with *tert*-Butyl-4-phenylbutaneperoxoate under irradiation. (bottom) mass spectrum of the product with the retention time of 5.4. This spectrum is different from that of an authentic sample of hexylbenzene (Figure S18).

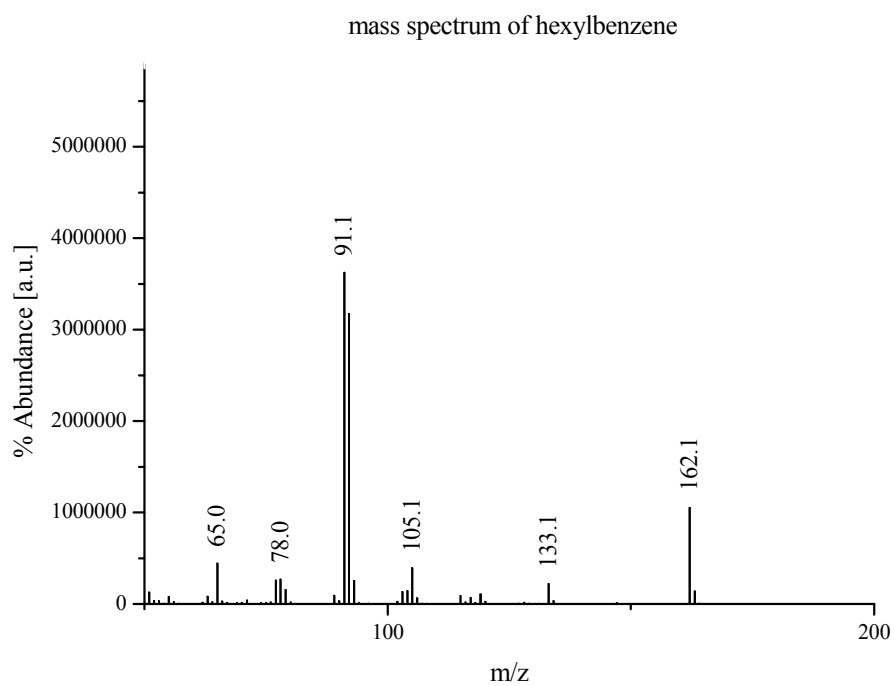
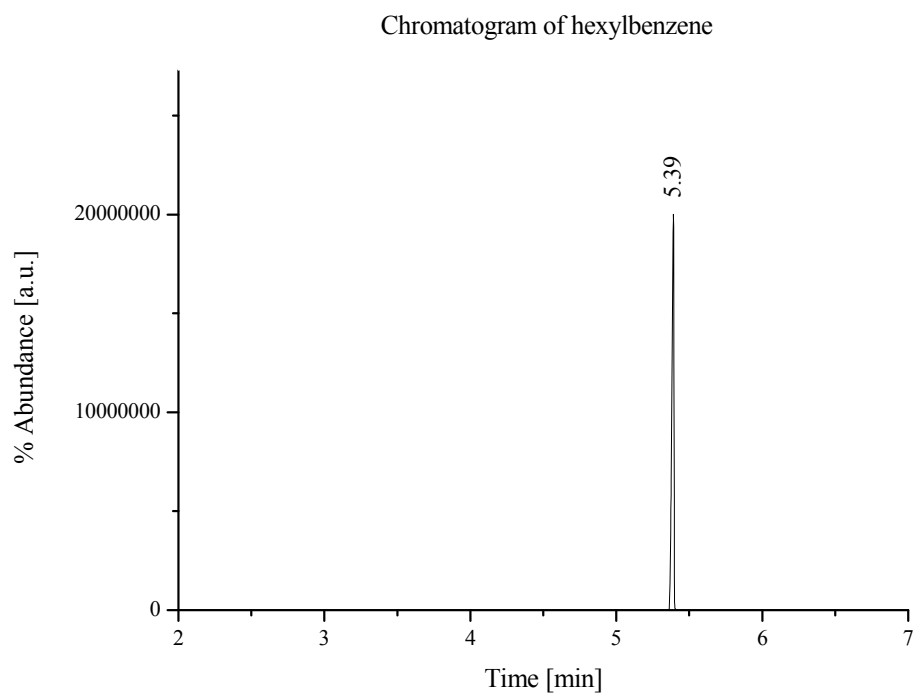


Figure S18. (top) Chromatogram and (bottom) mass spectrum of hexylbenzene.

Irradiation of [(N₂N)Ni- ⁿPr]

An air free NMR tube with septum screw cap was charged with [(N₂N)Ni- ⁿPr] (3.0 mg, 0.0084 mmol) in 0.5 mL of THF-d₈ inside the glovebox. The tube was transferred to the spectrometer and a ¹H NMR spectrum was recorded. The sample was ejected and placed in Rayonet Photochemical Reactor. After 2h a ¹H NMR spectrum was recorded, showing that no [(N₂N)Ni- ⁿPr] decomposed (still signal for α-CH₂ protons ~ -0.5 ppm). The NMR spectra are depicted in Figure S19.

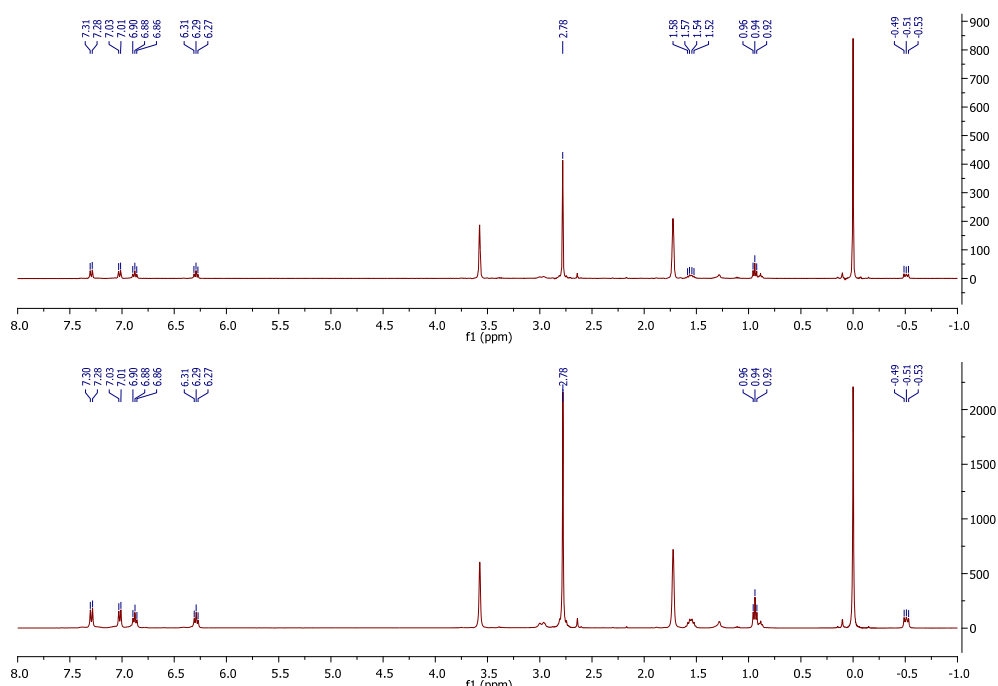


Figure S19. ¹H NMR (400 MHz, THF-d₈) of [(N₂N)Ni- ⁿPr] top before irradiation; bottom after irradiation.

Irradiation of *tert*-Butyl-4-phenylbutaneperoxoate

An air free NMR tube with septum screw cap was charged with *tert*-Butyl-4-phenylbutaneperoxoate (6.3 mg, 0.027 mmol) in 0.5 mL of THF-d₈ inside the glovebox. The tube was transferred to the spectrometer and a ¹H NMR spectrum was recorded. The sample was ejected and placed in Rayonet Photochemical Reactor. After 2h a ¹H NMR spectrum was recorded proving that all *tert*-Butyl-4-phenylbutaneperoxoate reacted. The NMR spectra are depicted in Figure S20. Then an aliquot (60 μL) was collected and transferred into a GC vial with 1 mL of Et₂O. The products were determined by GC-MS (Figure S21).

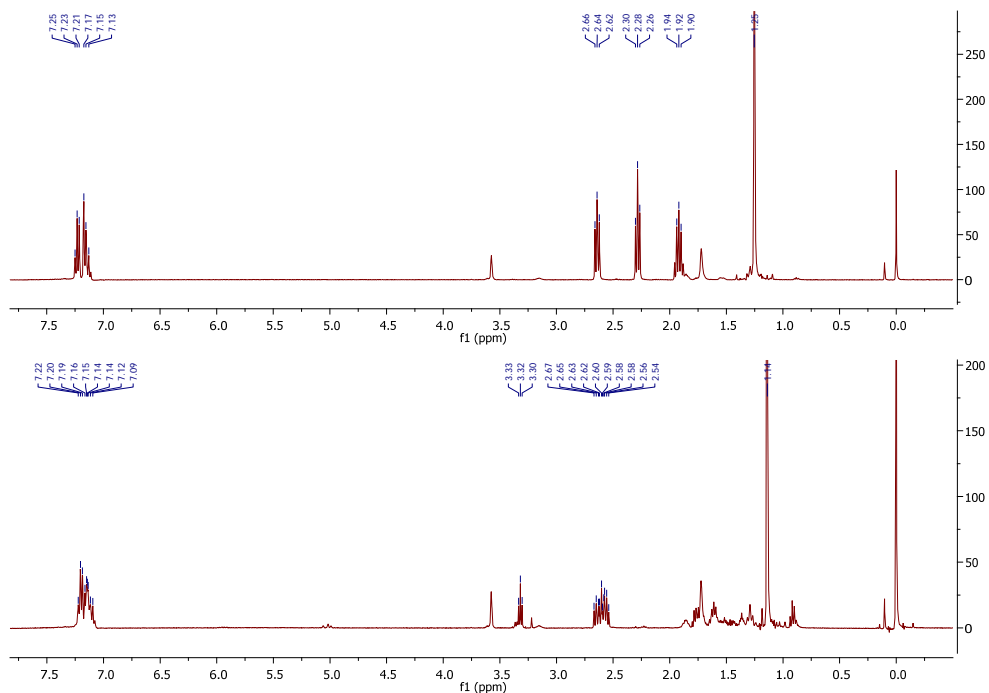


Figure S20. ¹H NMR (400 MHz, THF-d₈) of *tert*-Butyl-4-phenylbutaneperoxoate top before irradiation; bottom after irradiation.

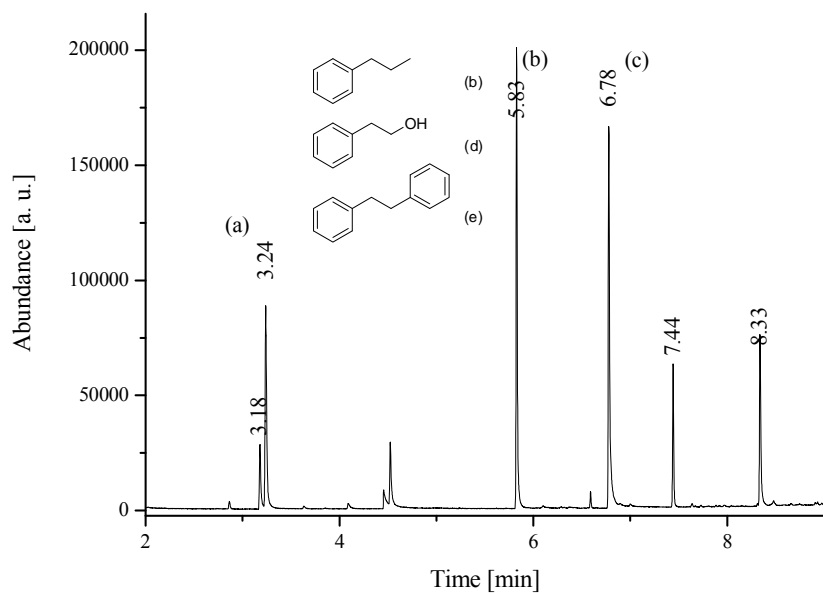


Figure S21. Chromatogram of *tert*-Butyl-4-phenylbutaneperoxoate after irradiation.

Resting state measurement

Prior to the experiments, the following standard solution was prepared: (A) [(N₂N)Ni- Cl] (174.3 mg, 0.498 mmol, 0.005 M) in 100 mL THF.

Inside the glovebox a brown glass vial was charged with C₈H₁₇I (120 mg, 0.5 mmol), C₁₂H₂₆ (50 mg, 0.294 mmol, internal standard), 3 mL of solution A (0.015 mmol, 3 mol% of [(N₂N)Ni-Cl]), 9 mL of DMA, a stirring bar. Then a Hellma Excalibur UV-vis fiber optic probe (connected to a Varian 50 Bio UV-Vis spectrometer) was introduced and the solution was cooled to -20°C.

When the temperature was equilibrated an aliquot (70 µL) was taken and transferred into a GC-MS vial (containing 100 µL CH₃CN). The measurement was launched (800 -350 nm, every 17 s, with a scanning rate of 2000 nm/min for 10 min) and EtMgCl (150 µL, 2M THF) was added at once. A GC sample was taken after 30 and 60 s (referring to addition of EtMgCl) and transferred into a GC-MS vial (containing 100 µL CH₃CN).

The obtained kinetic data (Figure S22) was smoothed and normalized. Then the absorption at 682 nm was analyzed. At this wave number the absorption of [(N₂N)Ni- Cl] (0.11608) and of [(N₂N)Ni- Et] (0.02346) are significantly different at the given concentration. With the assumption of a linear behavior of the absorption of [(N₂N)Ni- Cl] and [(N₂N)Ni- Et] at the given concentration we calculated their ratio. The GC-MS data we used to confirm that for the evaluated spectra the conversion of C₈H₁₇I has not reached its maximum (60% total would be expected based on C₈H₁₇I).

According to Figure S22, at a 25% conversion of octyl iodide (30 s after mixing), there is 63% of [(N₂N)Ni- Cl] remaining. At a 40% conversion of octyl iodide, there is 54% of [(N₂N)Ni- Cl] remaining. Additional data show that the concentration of [(N₂N)Ni- Cl] remains similar during catalysis (50-60% of initial value).

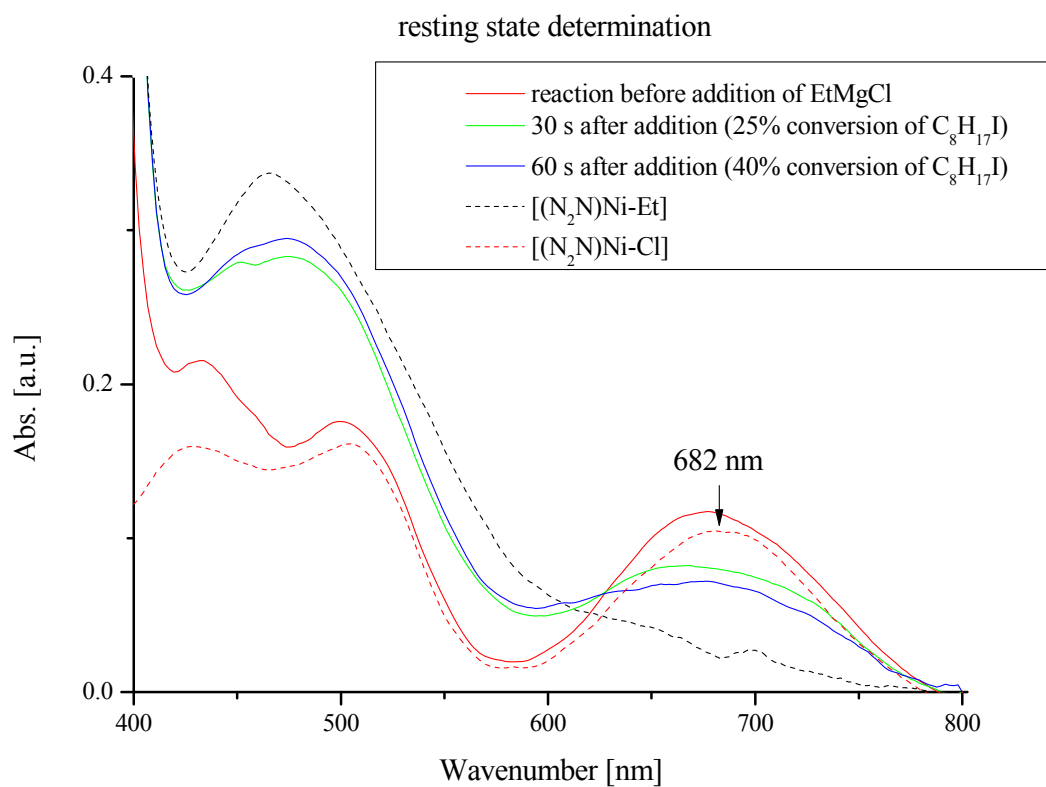


Figure S22. Absorption spectra of reaction mixture during a catalytic coupling of octyl iodide with $EtMgCl$.

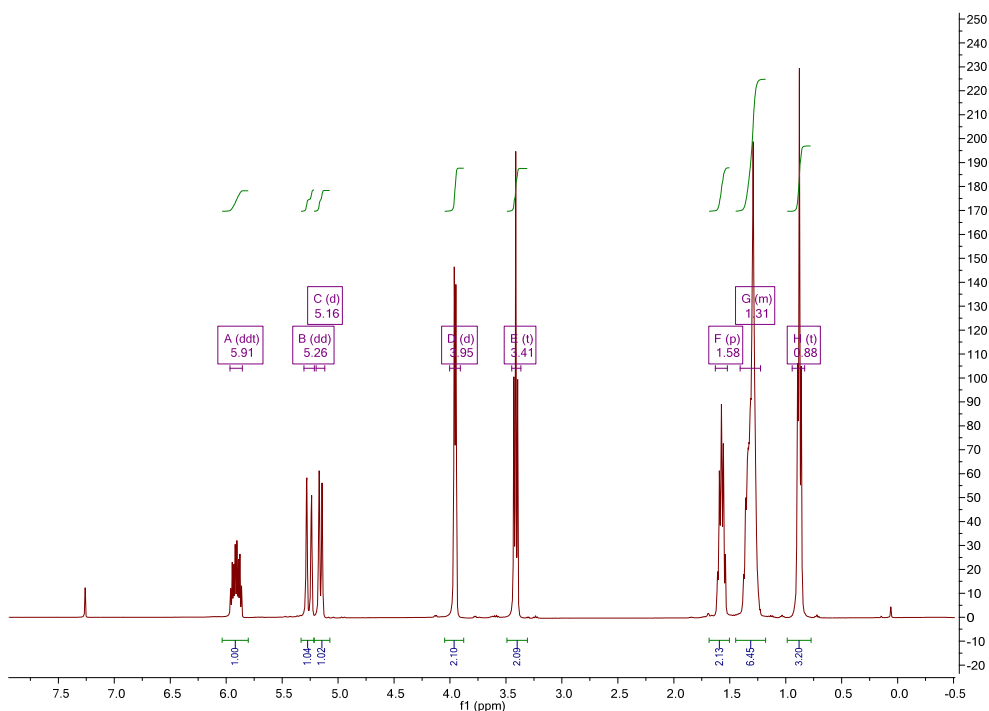


Figure S23. ^1H NMR (400 MHz, CDCl_3) spectrum of **12**.

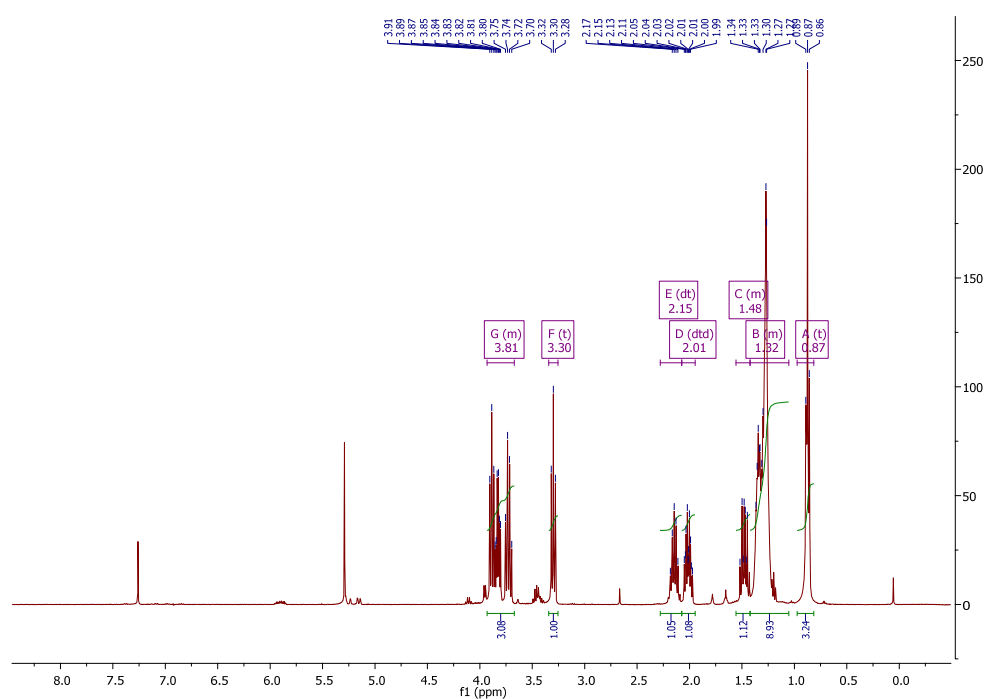


Figure S24. ^1H NMR (400 MHz, CDCl_3) spectrum of **13**.

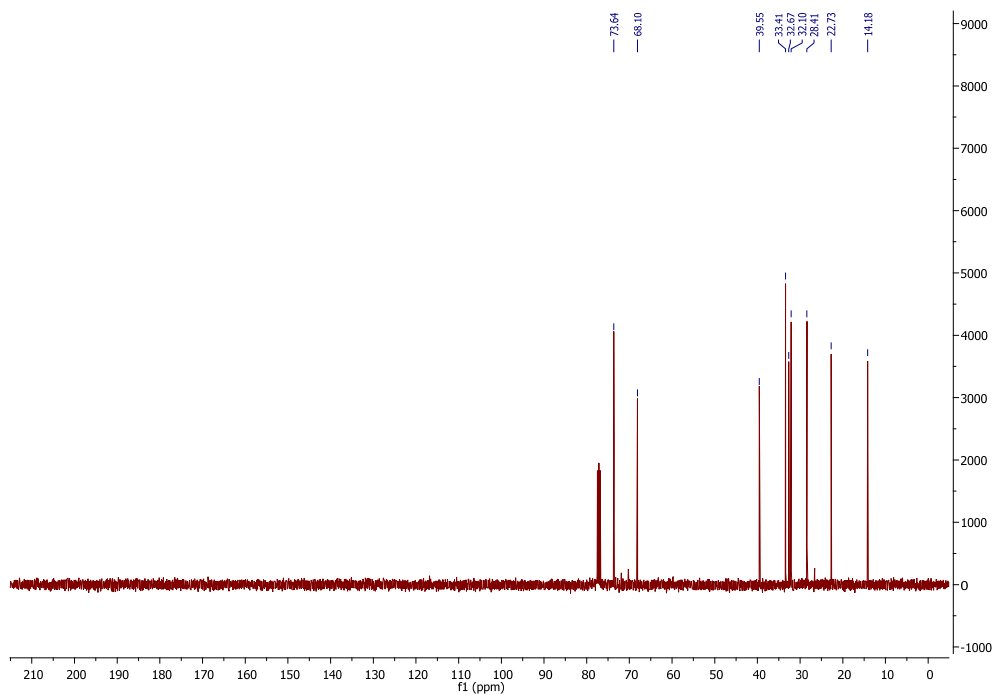


Figure S25. $^{13}\text{C}\{^1\text{H}\}$ NMR (100 MHz, CDCl_3) spectrum of **13**.

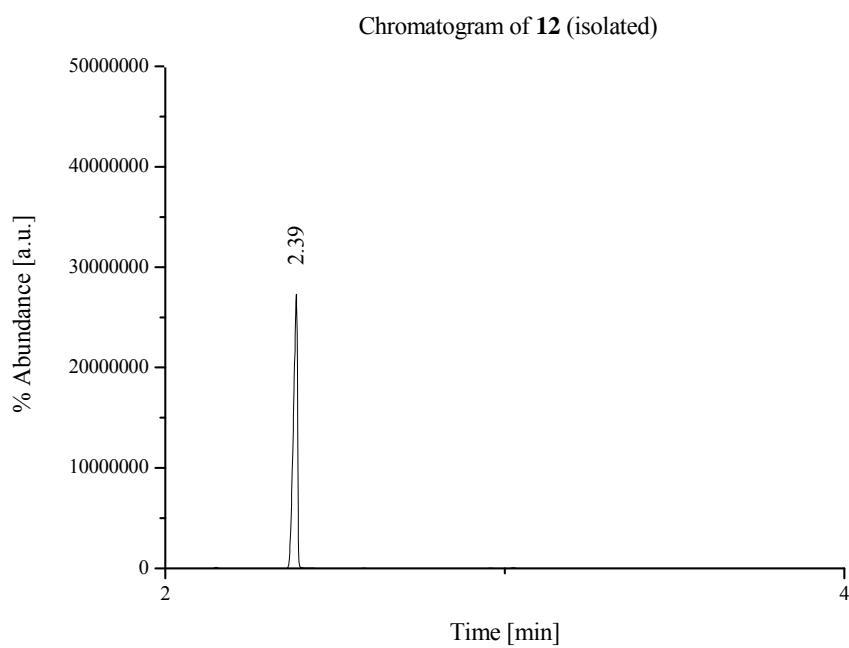


Figure S26. Chromatogram of the independently synthesized sample of **12**.

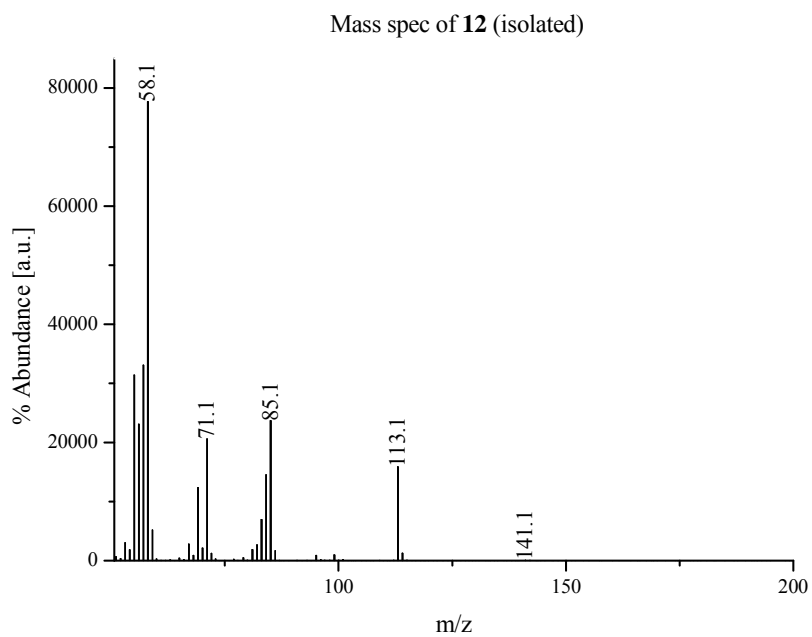


Figure S27. Mass spectrum of the independently synthesized sample of **12**.

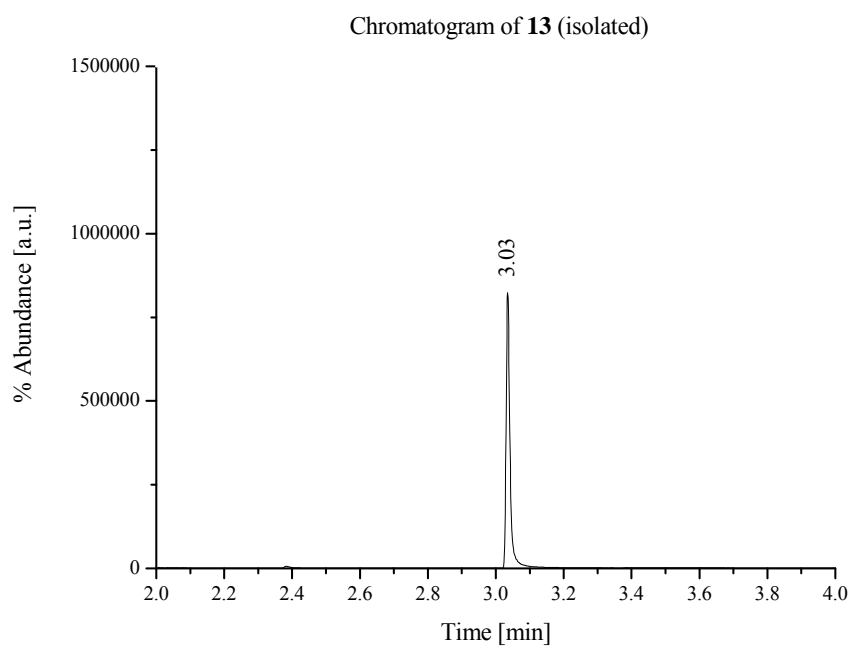


Figure S28. Chromatogram of the isolated sample of **13**.

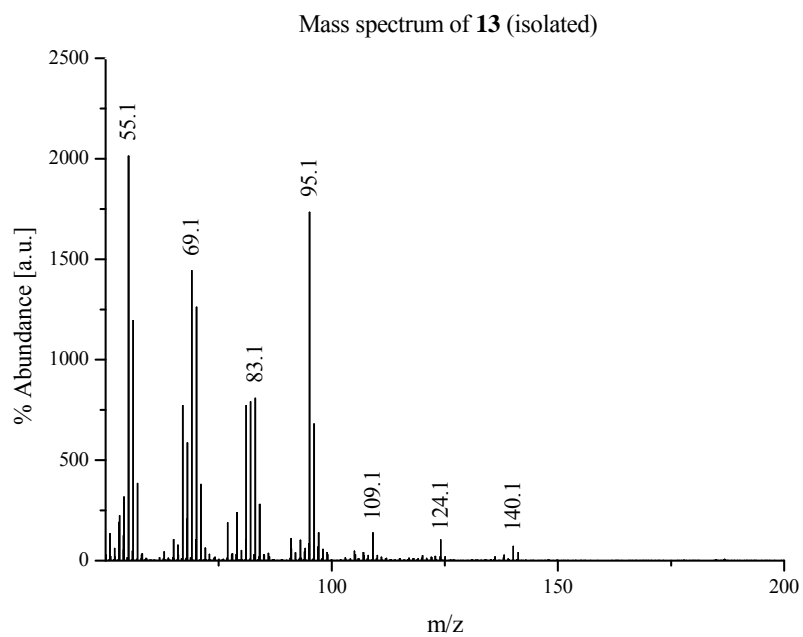


Figure S29. Mass spectrum of the isolated sample of **13**.

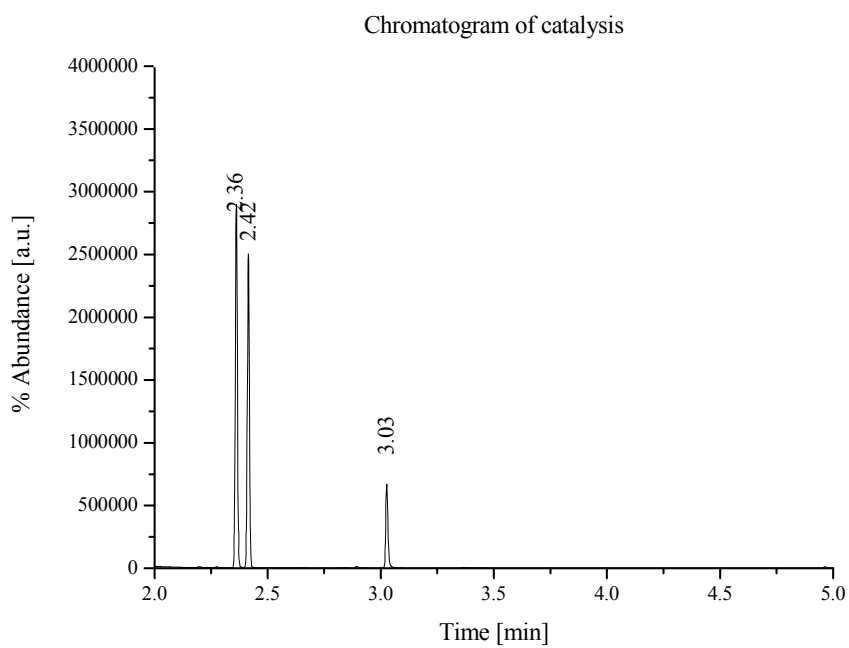


Figure S30. Chromatogram of the products from the coupling reactions shown in Scheme 2; both **12** and **13** can be identified by the retention time.

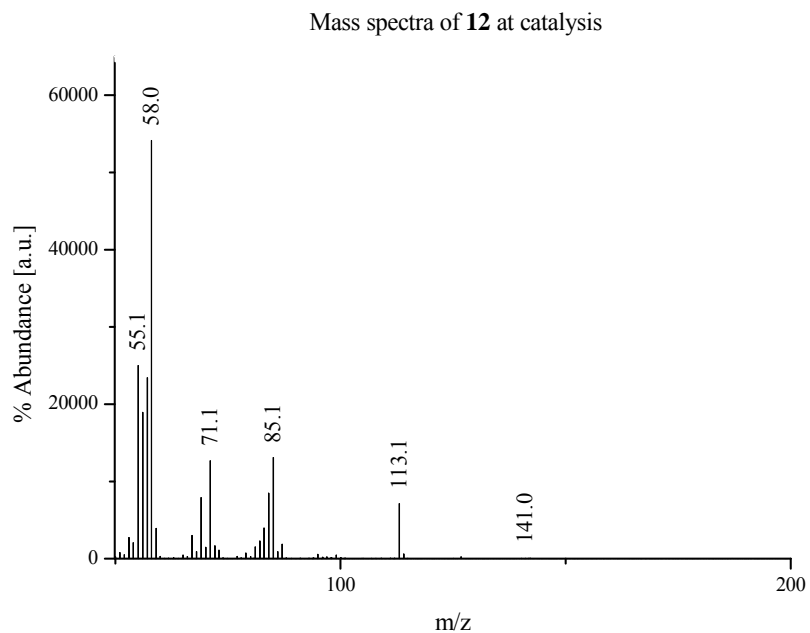


Figure S31. Mass spectrum of **12** produced from the coupling reactions shown in Scheme 2; the spectrum is identical to that of an independently prepared sample (Figure S27).

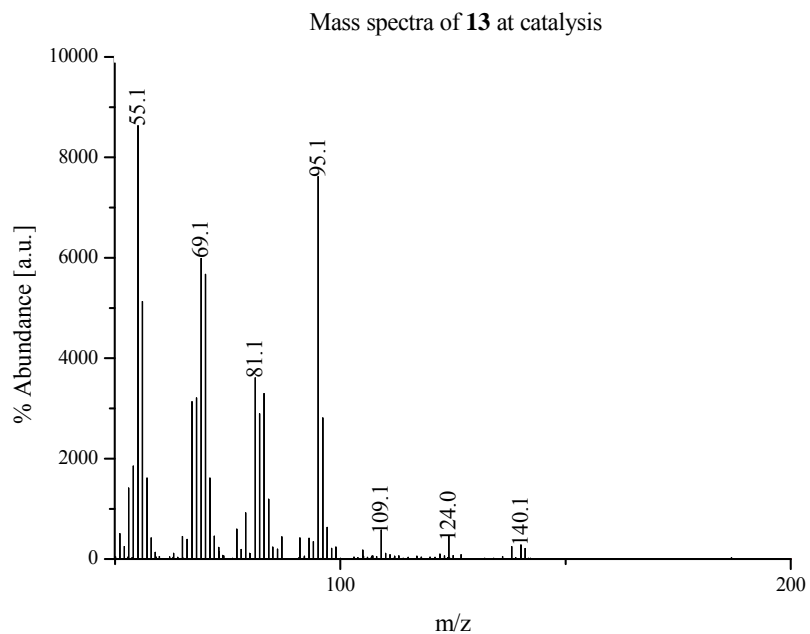


Figure S32. Mass spectrum of **13** produced from the coupling reactions shown in Scheme 2; the spectrum is identical to that of an isolated sample (Figure S29).

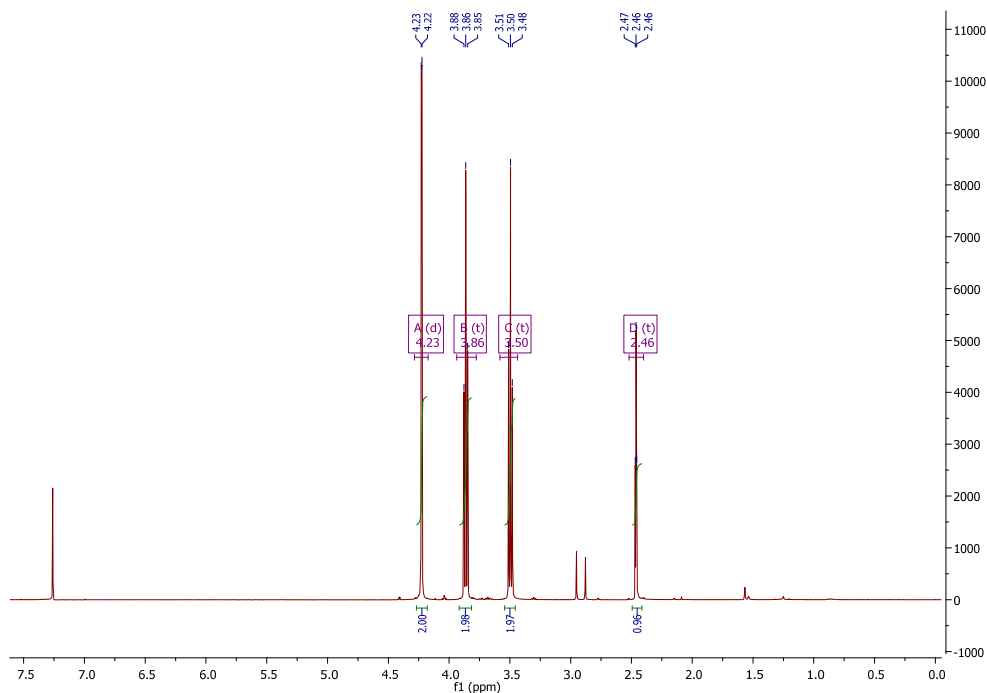


Figure S33. ^1H NMR (400 MHz, CDCl_3) spectrum of **22**.

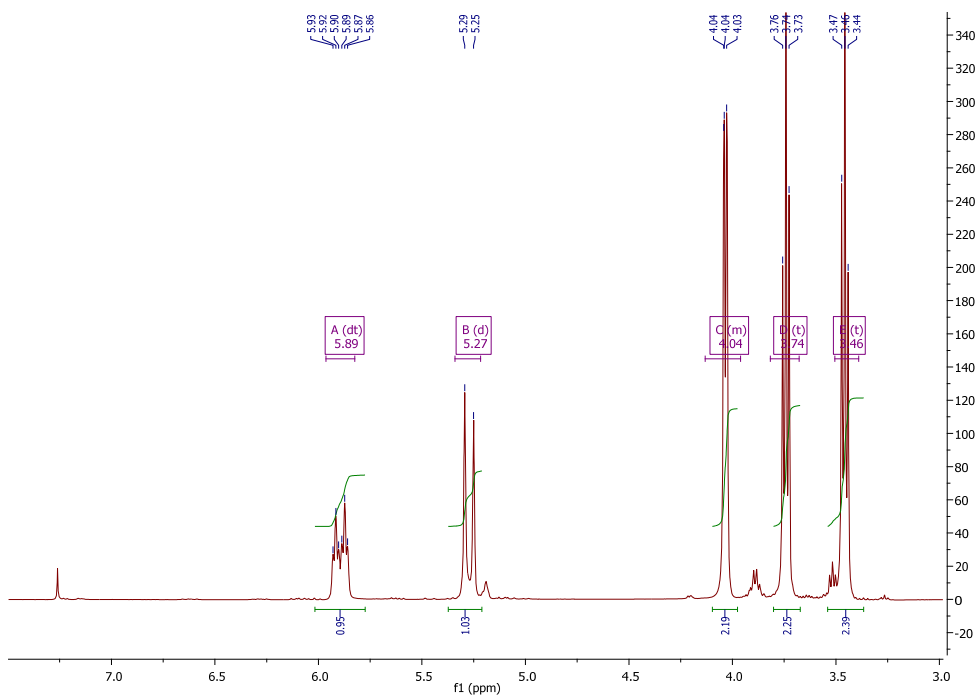


Figure S34. ^1H NMR (400 MHz, CDCl_3) spectrum of **9-D**.

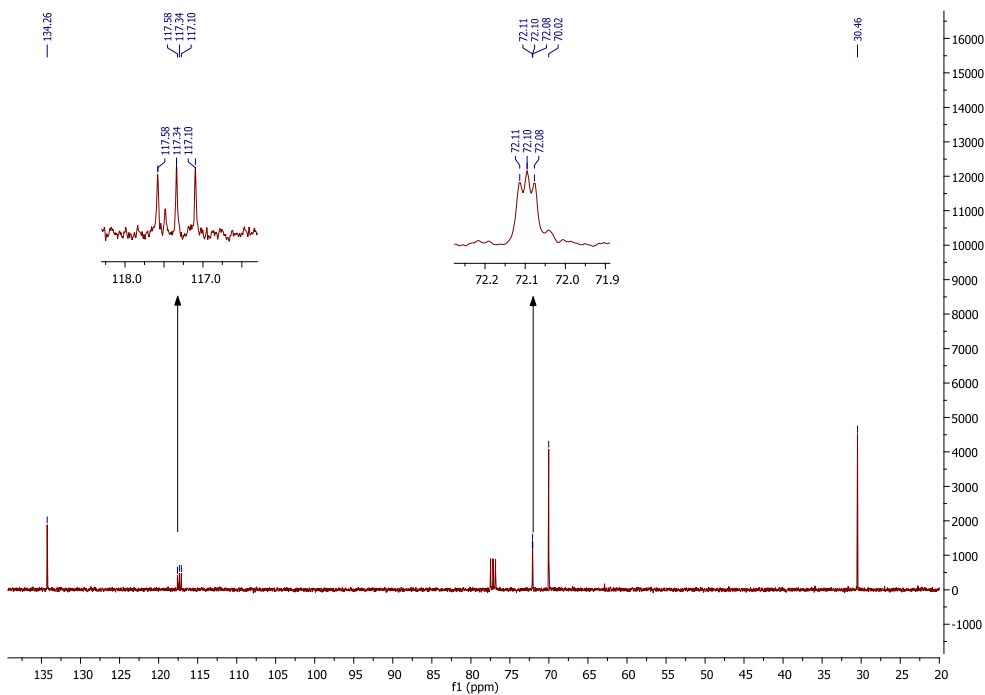


Figure S35. $^{13}\text{C}\{^1\text{H}\}$ NMR (100 MHz, CDCl_3) spectrum of **9-D**.

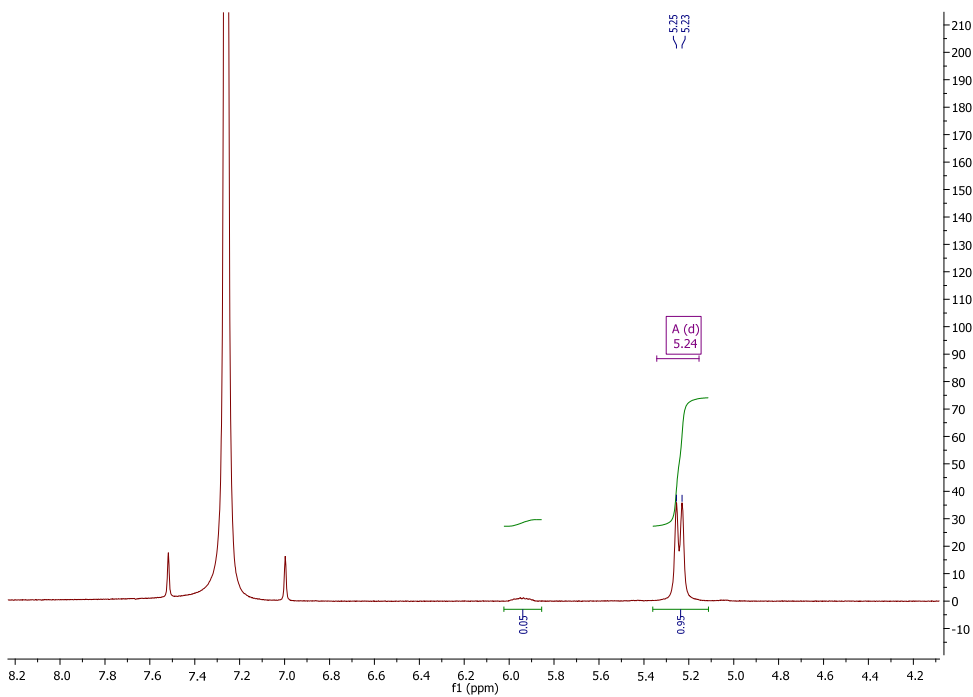


Figure S36. ^2H NMR (60 MHz, CDCl_3) spectrum of **9-D**.

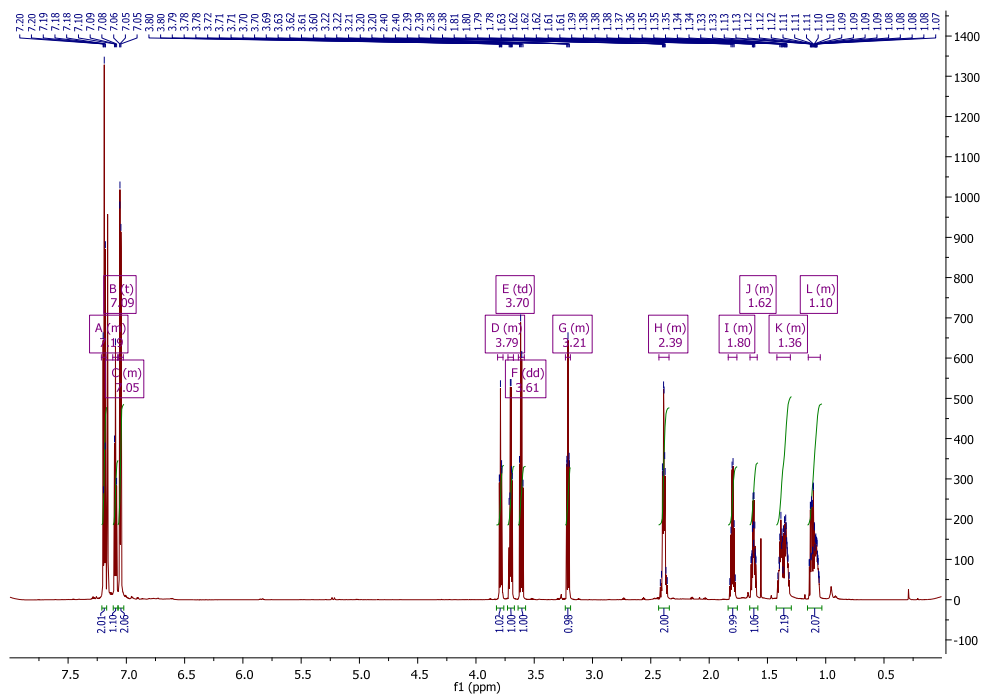


Figure S39. ^1H NMR (800 MHz, C_6D_6) spectrum of **14-D**.

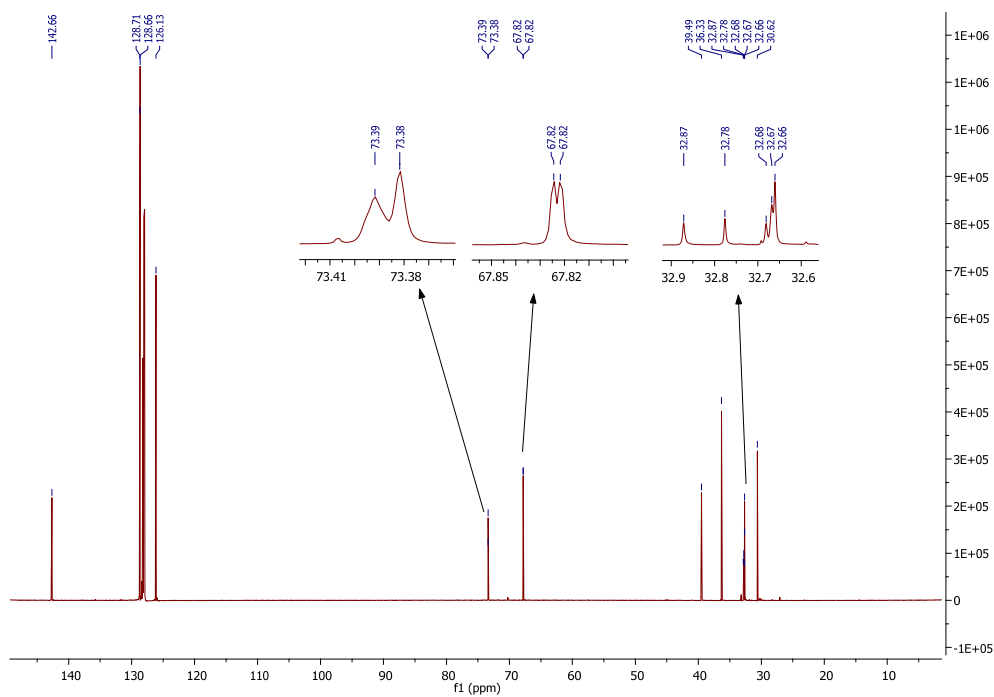


Figure S40. $^{13}\text{C}\{^1\text{H}\}$ NMR (200 MHz, C_6D_6) spectrum of **14-D** with expansion of signals showing diastereomers.

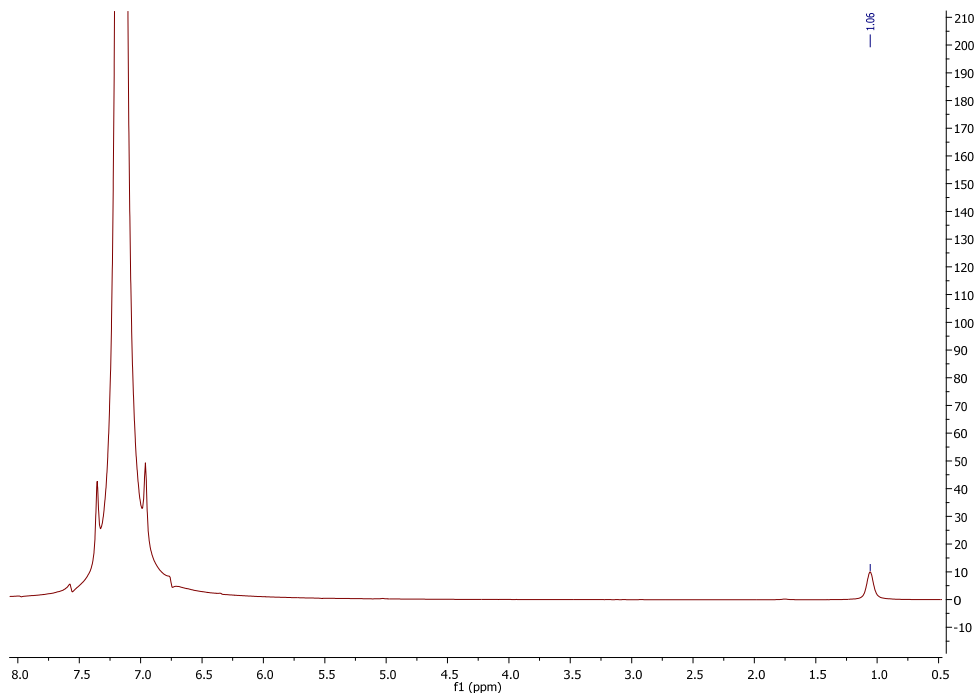


Figure S41. ^2H NMR (60 MHz, CDCl_3) spectrum of **14-D**.

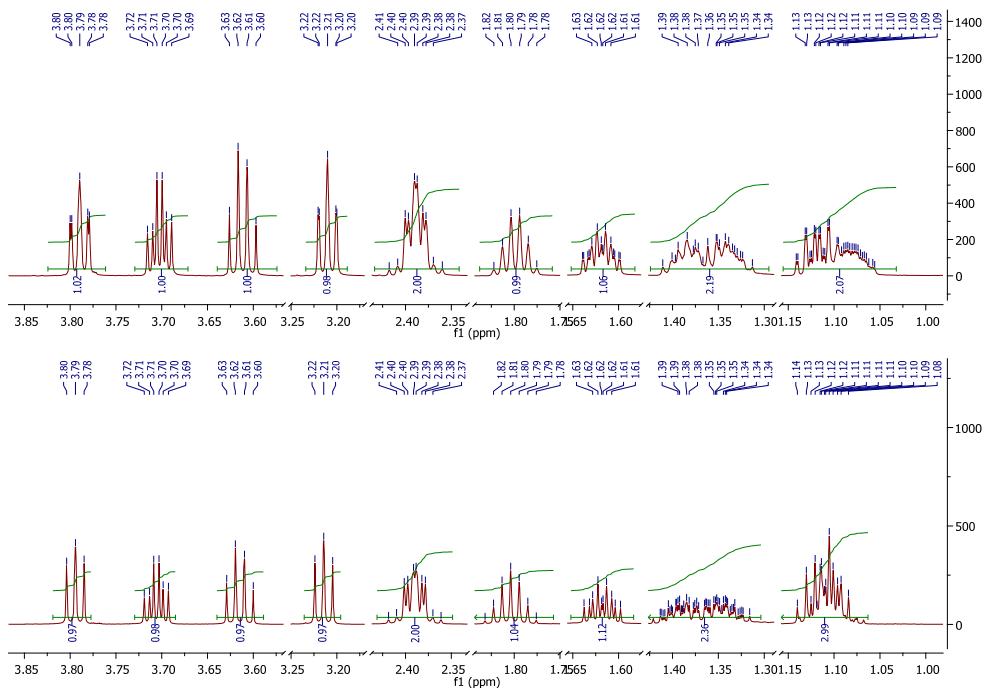


Figure S42. Expansion of ^1H NMR (800 MHz, C_6D_6) signals of **14-D** (top) and **14** (bottom).

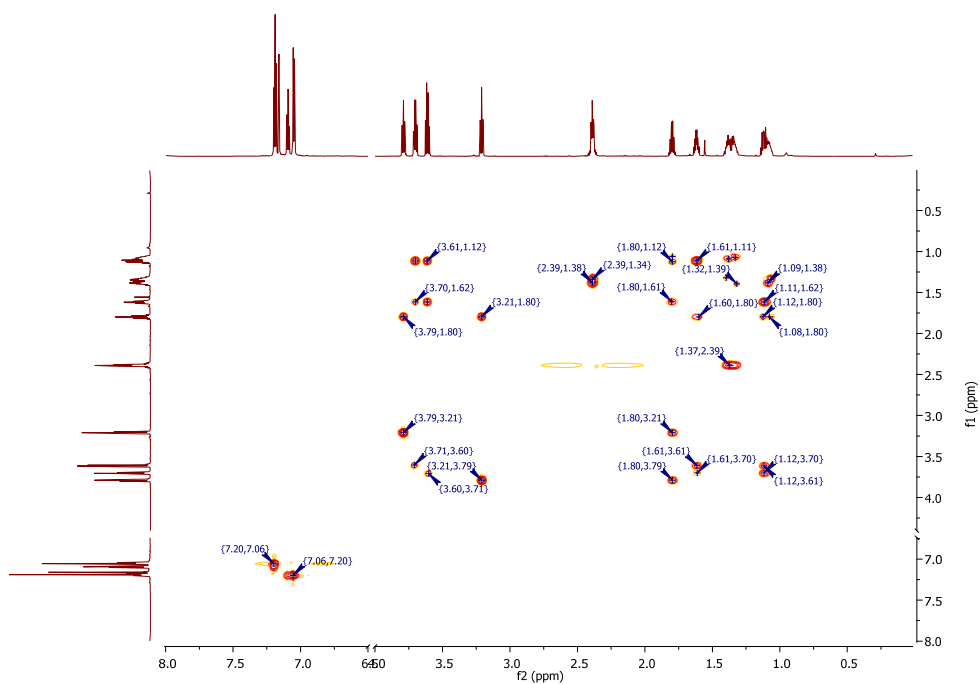


Figure S43. COSY NMR (800MHz, C₆D₆) spectrum of 14-D.

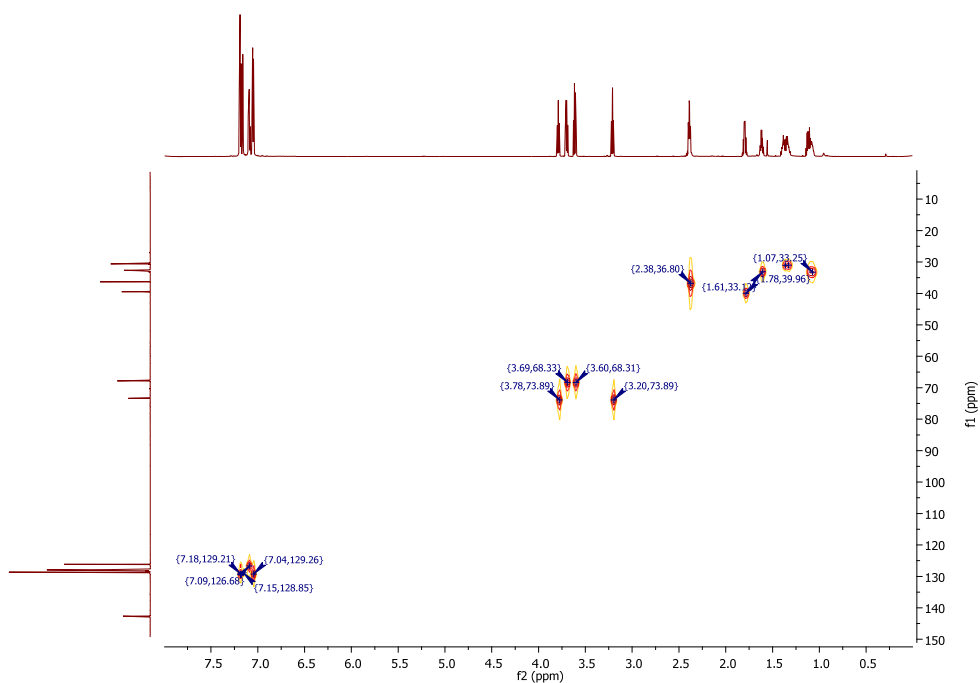


Figure S44. HMQC NMR (800MHz, C₆D₆) spectrum of 14-D.

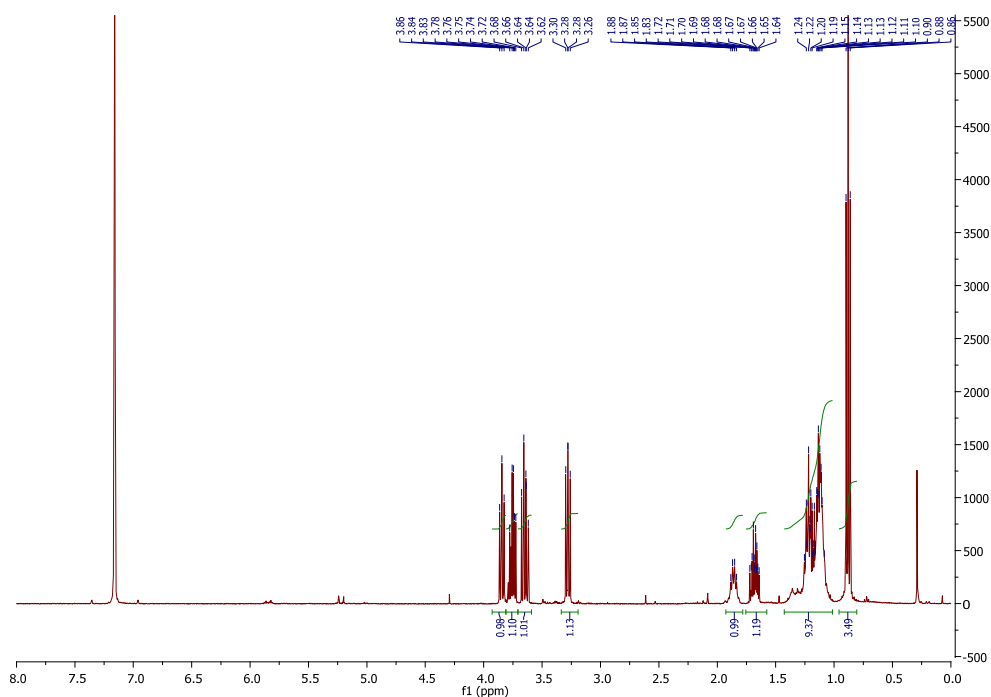


Figure S45. ^1H NMR (400 MHz, C_6D_6) spectrum of **13-D**.

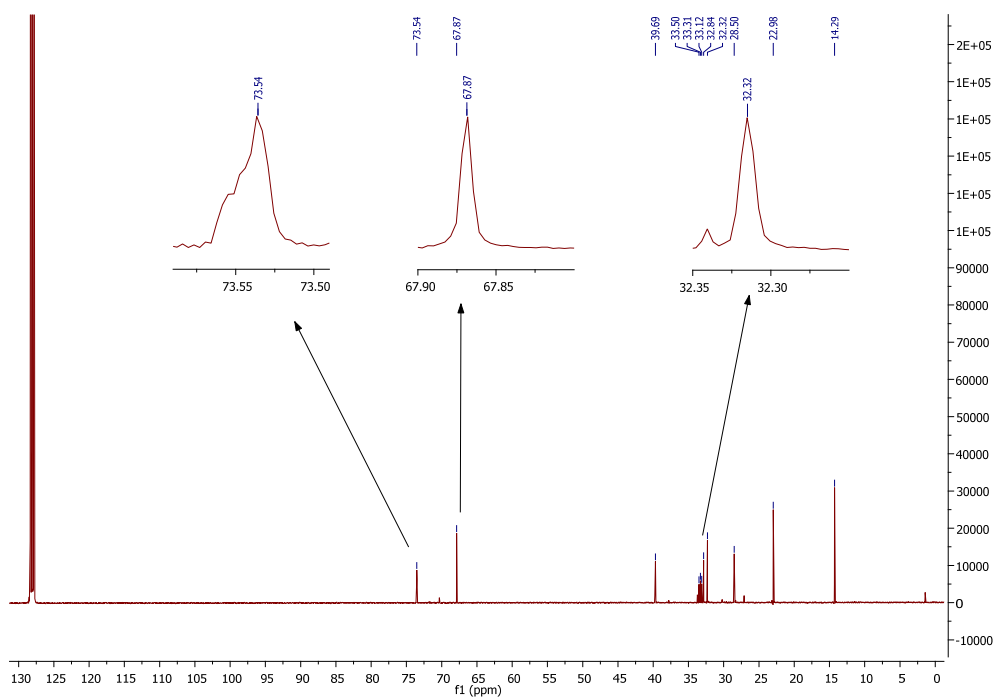


Figure S46. $^{13}\text{C}\{^1\text{H}\}$ NMR (100 MHz, C_6D_6) spectrum of **13-D** with expansion of broad signals indicating diastereomers.

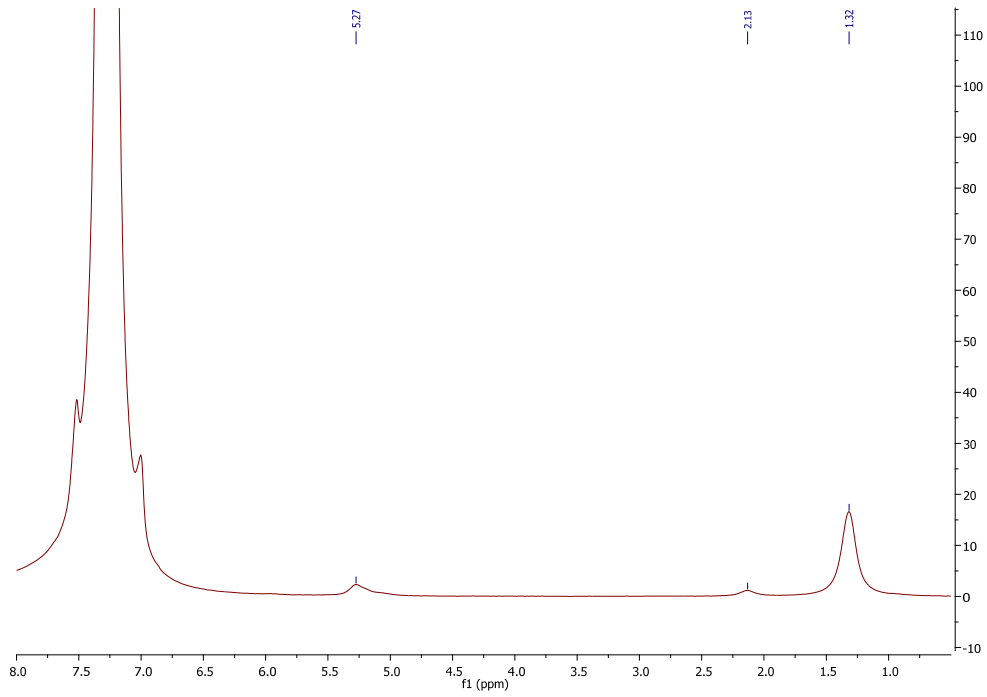


Figure S47. ^2H NMR (60 MHz, CDCl_3) spectrum of **13-D**.

Computational Details:

Geometry optimizations were performed at the M06^{12,13}/def2-SVP¹⁴ level using tetrahydrofuran as in implicit solvent within the SMD model¹⁵ and with the ultrafine integration grid in Gaussian09.¹⁶ Structures, and their associated energies, presented in the manuscript correspond to the lowest energy conformers, as determined by preliminary DFT computations. Structures **TS4,5** and **5** are open-shell singlets, and were computed using an unrestricted wavefunction. Refined energies were determined by single point computations at the M06/def2-TZVP level on M06/def2-SVP geometries. Free energies given in the manuscript include corrections taken from the M06/def2-SVP computations appended to M06/def2-TZVP//M06/def2-SVP energies. Basis sets were obtained from the EMSL website.

Attempts to locate a transition state associated with the **3**+Et•→**7** reaction were unsuccessful. Dissociation of the ethyl radical from **7** yielded an uphill curve, however, all energies on this curve were lower than the sum of the energies of **3** and the ethyl radical, indicating a barrierless reaction.

Table S1. Electronic and free energy corrections for relevant structures. Values in hartree.

Compound	M06/def2-SVP Electronic Energy	M06/def2-SVP Free Energy Correction	M06/def2-SVP Free Energy	M06/def2-TZVP Electronic Energy	M06/def2-TZVP Free Energy
Et•	-79.024031	0.034215	-78.989816	-79.115112	-79.080897
4	-4985.089296	0.370746	-4984.718550	-4986.591576	-4986.220830
TS4,5	-5064.096786	0.427623	-5063.669163	-5065.691707	-5065.264084
5	-5064.132318	0.430672	-5063.701646	-5065.726282	-5065.295610
3	-2411.301649	0.375499	-2410.92615	-2412.492443	-2412.116944
7	-2490.367189	0.433578	-2489.933611	-2491.639759	-2491.206181

Table S2. Reaction free energies at various theoretical levels. Values in kcal/mol.

Reaction	M06/def2-SVP	M06/def2-TZVP
4 + Et• → 5	4.22	3.84
4 + Et• → TS4,5	24.60	23.62
TS4,5 → 5	-20.38	-19.78
3 + Et• → 7	-11.07	-5.23

Molecular Geometries

COMPOUND 4

51

NiPincer - Br/Propyl

Ni	-0.50026	-0.43659	0.16445
C	2.08282	-1.49867	-0.61566
C	2.26425	-0.16373	-0.15096
C	3.56213	0.18698	0.27665
C	4.62762	-0.70273	0.16872
C	4.44197	-1.98108	-0.34796
C	3.15670	-2.37593	-0.72036
N	1.11999	0.59925	-0.07214
Br	-2.59335	-1.59291	-0.14862
N	0.73504	-1.90004	-0.92123
C	0.44369	-3.30162	-0.64077
C	1.04489	1.92428	0.28990
C	2.07596	2.88570	0.18664
C	1.89052	4.19785	0.60755
C	0.67281	4.61391	1.14101
C	-0.38349	3.70614	1.18151
C	-0.21765	2.39479	0.74555
N	-1.34468	1.49692	0.62399
C	-2.05707	1.79706	-0.62874
C	0.06114	-0.92601	1.98970
C	-0.91825	-1.70664	2.81484
C	-0.34420	-1.93407	4.20937
C	-2.26895	1.52112	1.75461
C	0.37397	-1.56752	-2.30546
H	2.99081	-3.39098	-1.09275
H	5.28053	-2.67680	-0.44068
H	5.61829	-0.38681	0.51082
H	3.74281	1.15779	0.73751
H	3.02843	2.61212	-0.26840
H	2.71846	4.90742	0.51074
H	0.53296	5.64081	1.48967
H	-1.36526	4.03374	1.53763
H	0.93736	-3.98387	-1.35855
H	-0.64363	-3.45826	-0.70561
H	0.77715	-3.55958	0.37634
H	0.55752	-0.49959	-2.50251
H	-0.69444	-1.77970	-2.47058
H	0.97381	-2.16303	-3.02116
H	-2.42671	2.84031	-0.63051
H	-2.90504	1.10748	-0.74979
H	-1.37712	1.66840	-1.48834
H	-1.71637	1.38951	2.69757
H	-2.83678	2.46886	1.81080
H	0.31006	0.05719	2.42792
H	0.98845	-1.48573	1.77166
H	-1.88045	-1.17298	2.89507
H	-1.14631	-2.67325	2.33478
H	-1.03822	-2.52406	4.83006
H	0.61438	-2.47871	4.17050
H	-0.15969	-0.97895	4.72995
H	-2.99158	0.69802	1.64079

COMPOUND TS4,5

58

NiPincer - Br/Propyl/Ethyl

C	2.11045	-1.50154	-0.59863
C	2.30050	-0.20445	-0.03844
C	3.59274	0.12294	0.42394
C	4.63307	-0.79712	0.34392
C	4.42541	-2.07072	-0.18420
C	3.15511	-2.41542	-0.65241
N	1.18114	0.55725	0.08765
Ni	-0.49063	-0.39106	-0.00253
Br	-1.76411	0.54580	-1.88216
N	0.79580	-1.77526	-1.15274
C	0.38427	-3.17774	-1.10296
C	1.04501	1.90722	0.24424
C	1.97870	2.87039	-0.18879
C	1.70299	4.23144	-0.09610
C	0.49339	4.67983	0.42865
C	-0.44075	3.74130	0.87369
C	-0.18384	2.37882	0.78639
N	-1.09713	1.38828	1.33349
C	-2.51785	1.70511	1.17740
C	-0.04191	-1.44125	1.62312
C	-1.34114	-2.01443	2.10337
C	-1.22016	-2.52754	3.53576
C	-0.81747	1.27470	2.77127
C	0.80547	-1.34907	-2.56474
H	2.98940	-3.40883	-1.08016
H	5.24368	-2.79417	-0.23748
H	5.62307	-0.51634	0.71790
H	3.76449	1.10176	0.88065
H	2.91528	2.53464	-0.64321
H	2.44547	4.95132	-0.45573
H	0.27219	5.74891	0.49329
H	-1.38865	4.08504	1.29995
H	1.00773	-3.81425	-1.75745
H	-0.65314	-3.25396	-1.46096
H	0.43892	-3.57595	-0.07924
H	1.07708	-0.28792	-2.64273
H	-0.19467	-1.47742	-3.00178
H	1.54067	-1.95605	-3.12696
H	-2.82768	2.54303	1.83019
H	-3.11386	0.82323	1.46806
H	-2.74149	1.94476	0.13022
H	0.25002	1.08571	2.95136
H	-1.08065	2.21927	3.28516
H	0.43059	-0.74665	2.32735
H	0.70004	-2.18839	1.30837
H	-2.14526	-1.25088	2.05800
H	-1.66619	-2.83413	1.43978
H	-2.16564	-2.97940	3.87651
H	-0.43233	-3.29470	3.61653
H	-0.96142	-1.71453	4.23482
H	-1.41540	0.46527	3.21950
C	-3.08411	-2.42468	-0.71286
H	-2.77435	-2.16603	-1.73134
H	-2.87134	-3.44960	-0.38201
C	-4.20396	-1.68031	-0.09835
H	-5.18534	-2.01732	-0.49270
H	-4.25458	-1.81649	0.99623
H	-4.13103	-0.60162	-0.32119

COMPOUND 5

58

NiPincer - Br/Propyl/Ethyl

C	2.33636	0.55038	-0.17067
C	1.45259	-0.29133	-0.90490
C	1.88588	-0.83318	-2.13533
C	3.13911	-0.51716	-2.63834
C	3.98582	0.33489	-1.92610
C	3.58444	0.86415	-0.69719
N	0.17414	-0.39860	-0.44092
Ni	-0.41436	1.15119	0.79947
Br	-1.27067	-0.45712	2.51414
N	1.88423	0.98075	1.11309
C	2.49458	2.21225	1.59631
C	-0.60582	-1.49584	-0.63148
C	-0.08667	-2.81204	-0.64753
C	-0.93759	-3.90255	-0.58828
C	-2.32149	-3.70699	-0.52999
C	-2.85588	-2.41908	-0.55102
C	-2.02122	-1.30615	-0.62421
N	-2.49500	0.01517	-0.74258
C	-3.79498	0.28388	-0.16634
C	-0.21250	2.53974	-0.58740
C	-1.30130	3.55417	-0.85828
C	-1.12143	4.24186	-2.20299
C	-2.39869	0.50679	-2.11083
C	2.08691	-0.08120	2.10994
H	4.26619	1.51524	-0.14438
H	4.97121	0.58949	-2.32651
H	3.45236	-0.91866	-3.60616
H	1.19408	-1.45089	-2.71615
H	0.99777	-2.95613	-0.62059
H	-0.52420	-4.91468	-0.55949
H	-2.99275	-4.56918	-0.47577
H	-3.94037	-2.28508	-0.52462
H	3.56220	2.07529	1.85613
H	1.97118	2.53506	2.50859
H	2.41355	3.01119	0.84492
H	1.61172	-1.01855	1.78937
H	1.62039	0.21410	3.06127
H	3.17020	-0.25468	2.26811
H	-4.63207	-0.16849	-0.73967
H	-3.96154	1.37417	-0.15444
H	-3.82227	-0.08003	0.87270
H	-1.38431	0.36648	-2.51559
H	-3.11033	-0.02413	-2.77867
H	-0.05996	1.91674	-1.48905
H	0.74339	3.05919	-0.38776
H	-2.30058	3.07541	-0.82801
H	-1.32581	4.32043	-0.06240
H	-1.88865	5.01402	-2.38324
H	-0.13475	4.73336	-2.27002
H	-1.17608	3.51920	-3.03682
H	-2.63710	1.58095	-2.14527
C	-0.79318	2.64249	2.00906
H	-0.29021	2.26686	2.91955
H	-0.28211	3.56867	1.69551
C	-2.25847	2.88166	2.27134
H	-2.41184	3.71060	2.99061
H	-2.81660	3.16212	1.36049
H	-2.74026	1.98526	2.69531

COMPOUND 3

50

NiPincer - Propyl

Ni	0.24506	-0.84352	-0.45248
C	-2.74338	2.05261	-0.11432
C	-1.88151	0.93081	-0.14961
C	-2.49642	-0.34438	-0.07689
C	-3.86759	-0.48750	0.09061
C	-4.69251	0.63518	0.17300
C	-4.11631	1.89790	0.04863
N	-0.52454	0.89827	-0.28741
C	1.06941	-2.59913	-0.46262
C	1.67207	-2.95694	0.88942
C	2.43527	-4.27247	0.89046
N	-1.62122	-1.50702	-0.27276
C	-1.94940	-2.11948	-1.57491
C	0.38057	1.91570	-0.18569
C	1.70978	1.54885	-0.52605
C	2.75382	2.46173	-0.46966
C	2.52892	3.77232	-0.04004
C	1.24195	4.14053	0.33980
C	0.18303	3.23866	0.27018
N	1.89864	0.16573	-0.97314
C	3.20405	-0.35799	-0.55486
C	1.80835	0.11595	-2.44793
C	-1.79521	-2.47897	0.81596
H	-4.31002	-1.48736	0.14481
H	-5.77115	0.51908	0.30950
H	-4.74946	2.79104	0.07270
H	-2.34514	3.05780	-0.25135
H	-0.79698	3.55960	0.62229
H	1.04938	5.15294	0.70995
H	3.35693	4.48477	0.00931
H	3.76503	2.15980	-0.75535
H	-2.99554	-2.47605	-1.59106
H	-1.28667	-2.97227	-1.77485
H	-1.82045	-1.37160	-2.37274
H	-1.54328	-2.00343	1.77578
H	-1.13593	-3.34265	0.65727
H	-2.83390	-2.85058	0.86331
H	4.02990	0.16691	-1.06519
H	3.28162	-1.42111	-0.81488
H	3.32428	-0.23844	0.53148
H	0.83708	0.51122	-2.77941
H	2.61367	0.72348	-2.90287
H	1.85965	-2.65604	-1.24214
H	0.35473	-3.40078	-0.74333
H	2.34880	-2.15525	1.24300
H	0.87393	-3.00502	1.65645
H	2.84316	-4.52819	1.88399
H	1.78829	-5.11016	0.57327
H	3.28477	-4.23846	0.18412
H	1.90881	-0.92359	-2.79462

COMPOUND 7

57

NiPincer - Propyl/Ethyl

C	1.48644	0.64561	-3.06503
C	0.52840	0.38076	-2.05543
C	-0.83334	0.33168	-2.47435
C	-1.19400	0.59900	-3.79038
C	-0.23366	0.90803	-4.75455
C	1.10816	0.90435	-4.37804
N	0.77359	0.09674	-0.74453
Ni	-0.76288	-0.16078	0.44655
C	-2.21997	-0.70907	1.59442
C	-2.45965	-0.26630	3.01988
C	-3.47188	-1.14032	3.74434
N	-1.81985	-0.09653	-1.49924
C	-2.15083	-1.50867	-1.70358
C	1.95720	0.24301	-0.06278
C	2.05677	-0.49324	1.15570
C	3.17448	-0.37628	1.97210
C	4.22382	0.48433	1.63227
C	4.13042	1.23130	0.46374
C	3.01951	1.11470	-0.37203
N	0.92711	-1.32030	1.50006
C	0.76958	-1.58186	2.92053
C	-1.06157	1.67609	1.00273
C	-0.14697	2.08263	2.12527
C	0.94596	-2.58931	0.76684
C	-3.02641	0.72215	-1.49939
H	-2.25039	0.55317	-4.07552
H	-0.53079	1.12791	-5.78374
H	1.88595	1.10670	-5.12213
H	2.54971	0.61988	-2.81972
H	2.95119	1.75761	-1.25196
H	4.92696	1.93315	0.19550
H	5.09451	0.57379	2.28821
H	3.23459	-0.95332	2.89907
H	-2.61615	-1.67928	-2.69497
H	-2.85726	-1.84963	-0.92944
H	-1.23652	-2.12269	-1.64497
H	-2.76059	1.78592	-1.41016
H	-3.66531	0.44799	-0.64561
H	-3.62817	0.58592	-2.41871
H	1.55966	-2.24897	3.32008
H	-0.19587	-2.08464	3.09200
H	0.78402	-0.63971	3.48982
H	1.06092	-2.41012	-0.31187
H	1.78116	-3.23322	1.10867
H	-1.95361	-1.79450	1.57200
H	-3.15876	-0.59562	1.01665
H	-1.51542	-0.26344	3.59501
H	-2.81381	0.78190	3.03295
H	-3.66470	-0.79059	4.77268
H	-4.44032	-1.15804	3.21394
H	-3.12242	-2.18631	3.81209
H	0.00105	-3.13384	0.93522
H	-2.12090	1.87297	1.23351
H	-0.80398	2.19218	0.05850
H	-0.25402	3.16060	2.35695
H	-0.36295	1.54273	3.06374
H	0.91872	1.92105	1.88383

References

- (1) Csok, Z.; Vechorkin, O.; Harkins, S. B.; Scopelliti, R.; Hu, X. L. *J. Am. Chem. Soc.* **2008**, *130*, 8156-8157.
- (2) Breitenfeld, J.; Vechorkin, O.; Corminboeuf, C.; Scopelliti, R.; Hu, X. L. *Organometallics* **2010**, *29*, 3686-3689.
- (3) Kinney, R. J.; Jones, W. D.; Bergman, R. G. *J. Am. Chem. Soc.* **1978**, *100*, 7902-15.
- (4) Nieman, J. A.; Nair, S. K.; Heasley, S. E.; Schultz, B. L.; Zerth, H. M.; Nugent, R. A.; Chen, K.; Stephanski, K. J.; Hopkins, T. A.; Knechtel, M. L.; Oien, N. L.; Wieber, J. L.; Wathen, M. W. *Bioorg. Med. Chem. Lett.* **2010**, *20*, 3039-3042.
- (5) Mayer, T.; Maier, M. E. *Eur. J. Org. Chem.* **2007**, *2007*, 4711-4720.
- (6) Rueda-Becerril, M.; Chatalova Sazepin, C.; Leung, J. C. T.; Okbinoglu, T.; Kennepohl, P.; Paquin, J.-F. o.; Sammis, G. M. *J. Am. Chem. Soc.* **2012**, *134*, 4026-4029.
- (7) Love, B. E.; Jones, E. G. *J. Org. Chem.* **1999**, *64*, 3755-3756.
- (8) Su, C.-C.; Williard, P. G. *Org. Lett.* **2010**, *12*, 5378-5381.
- (9) Creutz, S. E.; Lotito, K. J.; Fu, G. C.; Peters, J. C. *Science* **2012**, *338*, 647-651.
- (10) Warren, S. C.; Messina, L. C.; Slaughter, L. S.; Kamperman, M.; Zhou, Q.; Gruner, S. M.; DiSalvo, F. J.; Wiesner, U. *Science* **2008**, *320*, 1748-1752.
- (11) Tang, H.; Richey, H. G., Jr. *Organometallics* **2001**, *20*, 1569-1574.
- (12) Zhao, Y.; Truhlar, D. G. *Theor. Chem. Acc.* **2008**, *120*, 215.
- (13) Zhao, Y.; Truhlar, D. G. *Acc. Chem. Res.* **2008**, *41*, 157.
- (14) Schafer, A.; Horn, H.; Ahlrichs, R. *J. Chem. Phys.* **1992**, *97*, 2571.
- (15) Marenich, A. V.; Cramer, C. J.; Truhlar, D. G. *J. Phys. Chem. B* **2009**, *113*, 6378.
- (16) Frisch, M. J.; Trucks, G. W.; Schlegel, H. B.; Scuseria, G. E.; Robb, M. A.; Cheeseman, J. R.; Scalmani, G.; Barone, V.; Mennucci, B.; Petersson, G. A.; Nakatsuji, H.; Caricato, M.; Li, X.; Hratchian, H. P.; Izmaylov, A. F.; Bloino, J.; Zheng, G.; Sonnenberg, J. L.; Hada, M.; Ehara, M.; Toyota, K.; Fukuda, R.; Hasegawa, J.; Ishida, M.; Nakajima, T.; Honda, Y.; Kitao, O.; Nakai, H.; Vreven, T.; Montgomery, J., J. A.; Peralta, J. E.; Ogliaro, F.; Bearpark, M.; Heyd, J. J.; Brothers, E.; Kudin, K. N.; Staroverov, V. N.; Kobayashi, R.; Normand, J.; Raghavachari, K.; Rendell, A.; Burant, J. C.; Iyengar, S. S.; Tomasi, J.; Cossi, M.; Rega, N.; Millam, M. J.; Klene, M.; Knox, J. E.; Cross, J. B.; Bakken, V.; Adamo, C.; Jaramillo, J.; Gomperts, R.; Stratmann, R. E.; Yazyev, O.; Austin, A. J.; Cammi, R.; Pomelli, C.; Ochterski, J. W.; Martin, R. L.; Morokuma, K.; Zakrzewski, V. G.; Voth, G. A.; Salvador, P.; Dannenberg, J. J.; Dapprich, S.; Daniels, A. D.; Farkas, O.; Foresman, J. B.; Ortiz, J. V.; Cioslowski, J.; Fox, D. J.; Gaussian, Inc.: Wallingford, CT, 2009.